

INVESTIGATION OF THE LIMITS OF INERTIAL SUPPORT
IMPLEMENTATION AND THE EFFECTS OF SYNTHETIC INERTIA IN
VARIABLE SPEED WIND TURBINES

A THESIS SUBMITTED TO
THE GRADUATE SCHOOL OF NATURAL AND APPLIED SCIENCES
OF
MIDDLE EAST TECHNICAL UNIVERSITY

BY

ERENCAN DUYMAZ

IN PARTIAL FULFILLMENT OF THE REQUIREMENTS
FOR
THE DEGREE OF MASTER OF SCIENCE
IN
ELECTRICAL AND ELECTRONICS ENGINEERING

DECEMBER 2018

Approval of the thesis:

**INVESTIGATION OF THE LIMITS OF INERTIAL SUPPORT
IMPLEMENTATION AND THE EFFECTS OF SYNTHETIC INERTIA IN
VARIABLE SPEED WIND TURBINES**

submitted by **Erencan Duymaz** in partial fulfillment of the requirements for the degree of **Master of Science in Electrical and Electronics Engineering Department, Middle East Technical University** by,

Prof. Dr. Gülbil Dural Ünver _____
Dean, Graduate School of **Natural and Applied Sciences**

Prof. Dr. Bölüm Başkanı _____
Head of Department, **Electrical and Electronics Engineering**

Ozan KEYSAN _____
Supervisor, **Department of Electrical and Electronics Engineering, METU**

Examining Committee Members:

Prof. Dr. Jüri _____
JüriBölüm, METU

Prof. Dr. Jüri _____
JüriBölüm, METU

Prof. Dr. Jüri _____
JüriBölüm, METU

Assoc. Prof. Dr. Jüri _____
JüriBölüm, METU

Assist. Prof. Dr. Jüri _____
JüriBölüm, Ankara University

Date: _____

I hereby declare that all information in this document has been obtained and presented in accordance with academic rules and ethical conduct. I also declare that, as required by these rules and conduct, I have fully cited and referenced all material and results that are not original to this work.

Name, Last Name: Erencan Duymaz

Signature : 

ABSTRACT

INVESTIGATION OF THE LIMITS OF INERTIAL SUPPORT IMPLEMENTATION AND THE EFFECTS OF SYNTHETIC INERTIA IN VARIABLE SPEED WIND TURBINES

Duymaz, Erençan

M.S., Department of Electrical and Electronics Engineering
Supervisor : Ozan KEYSAN

December 2018, 67 pages

The share of renewable energy systems in the installed capacity increases dramatically. Research shows that increase in the renewable energy percentage brings power system stability problems due to the decrease in the grid aggregated inertia. To prevent the decrease in the grid inertia, renewable energy systems can be equipped with the provision of inertial support that is the inherited behaviour of the conventional synchronous generators. Especially, wind turbines are able to provide additional amount of active power in the frequency disturbances by extracting the kinetic energy stored in the turbine and generator inertia. The inertial support implementation is studied for a variable speed wind turbine with a full scale power electronic. The limits of inertial support is also investigated by considering the extreme conditions such as low wind speed or high wind speed. The maximum achievable active power is found out to be limited by the wind speed and no recovery state is required for high wind speeds. Moreover, the synthetic inertia implementation for a variable speed wind turbine is presented. The effect of the implementation in the P.M.Anderson test case is observed for different inertia constants. It is also validated that higher inertia

constant synthetic inertia implementation possess the ability to lower RoCoF following a frequency disturbance especially in the cases where the conventional power plants are decommissioned and the power grid has low rotational inertia.

Keywords: Güç Sistemleri Frekans Stabilitesi, Atalet Desteği, Yapay Atalet, Sanal Atalet, Yenilebilir Enerji

ÖZ

BAŞLIK

Duymaz, Erencan

Yüksek Lisans, Elektrik ve Elektronik Mühendisliği Bölümü

Tez Yöneticisi : Ozan KEYSAN

Aralık 2018 , 67 sayfa

Kurulu güçteki yenilenebilir enerji oranı önemli ölçüde artmaktadır. Araştırmalara göre yenilenebilir enerji oranındaki artış şebekenin toplu ataletindeki düşüşten kaynaklanan güç sistemleri stabilite sorunlarını da beraberinde getirmektedir.

Anahtar Kelimeler: Power System Frequency Stability, Inertial Support, Synthetic Inertia, Virtual Inertia, Renewable Energy

To my precious mom...

ACKNOWLEDGMENTS

Teşekkür edilecekler

TABLE OF CONTENTS

ABSTRACT	v
ÖZ	vii
ACKNOWLEDGMENTS	ix
TABLE OF CONTENTS	x
LIST OF TABLES	xiv
LIST OF FIGURES	xv
LIST OF ABBREVIATIONS	xix
LIST OF SYMBOLS	xx
CHAPTERS	
1 INTRODUCTION	1
1.1 Global Renewable Energy Status	1
1.1.1 EU 2020 Goals	3
1.1.2 Wind Energy Status	4
1.2 Global Renewable Energy Future	5
1.3 Renewable Energy Problems	6
1.4 Literature Review	10
1.5 Thesis Motivation	11

1.6	Thesis Outline	11
2	POWER SYSTEM FREQUENCY STABILITY	13
2.1	Synchronous Generator and Synchronous Speed	13
2.2	Swing Equation	14
2.3	Frequency in Power Systems	15
2.3.1	Primary Frequency Control	16
2.3.2	Secondary and Tertiary Control	17
3	WIND TURBINE MODELLING	19
3.1	Variable Speed PMSG Wind Turbines	19
3.1.1	Aerodynamic Model	20
3.1.1.1	Maximum Power Point Tracking Algorithms	21
3.1.1.2	Pitch Angle Control	22
3.1.2	Gearbox	24
3.1.3	Permanent Magnet Synchronous Generator	25
3.1.4	Machine Side Converter	26
3.1.5	Grid Side Converter	27
3.2	Synthetic Inertia Implementation	29
3.2.1	Synthetic Inertia Activation Schemes	30
3.2.2	Source of the Inertial Support	31
4	INVESTIGATION OF INERTIAL SUPPORT PRACTICAL LIMITS	33
4.1	Inertial Support Limits	33
4.2	Inertial Support Under Different Wind Speeds	35

4.2.1	Low Wind Scenario	36
4.2.1.1	Active Power Limit in Low Wind Scenario	36
4.2.1.2	Active Power in Low Wind Scenario .	37
4.2.2	Medium Wind Scenario	39
4.2.2.1	Active Power in Medium Wind Scenario	40
4.2.2.2	Generator Speed, Turbine and Generator Torques in Medium Wind Scenario	41
4.2.2.3	DC-Link Voltage in Medium Wind Scenario	41
4.2.3	High Wind Scenario	42
4.2.3.1	Active Power in High Wind Scenario .	44
4.2.3.2	Generator Speed, Turbine and Generator Torques in High Wind Scenario .	44
4.2.3.3	DC-Link Voltage in High Wind Scenario	45
4.3	Probabilistic Approach for Different Wind Speeds	47
5	VALIDATION IN TEST CASE	49
5.1	P.M.Anderson 9 Bus Test Case	49
5.1.1	System Properties	49
5.1.2	Load Flow Analysis for Base Case	50
5.1.3	Base Case Frequency Response for Additional Load Connection	51
5.2	Modified Case	54
5.2.1	Load Flow Analysis for Modified Case	54
5.2.2	Modified Case Frequency Response for Additional Load Connection	55

5.3	Decommissioned Case	57
5.3.1	Load Flow Analysis for Decommissioned Case . .	57
5.3.2	Decommissioned Case Frequency Response for Ad- ditional Load Connection	58
6	EVALUATION OF FAST INERTIAL RESPONSE AND SYNTHETIC INERTIA IMPLEMENTATION	61
6.1	FAST INERTIAL RESPONSE	61
6.2	SYNTHETIC INERTIA IMPLEMENTATION	61
6.3	FUTURE WORK	61
	REFERENCES	63
	APPENDICES	
A	EK A	67
A.1	Örnek Kısım	67

LIST OF TABLES

TABLES

Table 1.1 Comparison of Different Type of Generators for Inertial Response Behaviour	9
Table 5.1 Generator Properties of Test System	49
Table 5.2 Load Properties of Test System	50
Table 5.3 Load Flow Results in Base Case	51
Table 5.4 System Dynamical Properties	51
Table 5.5 Load Flow Results for Modified Case	55
Table 5.6 System Dynamical Properties	58
Table 5.7 Load Flow Results for Decommissioned Case	58

LIST OF FIGURES

FIGURES

Figure 1.1 Installed Renewable Energy Capacity of Leading Countries	1
Figure 1.2 Renewable Energy Production of Leading Countries	2
Figure 1.3 Average Renewable Energy Generation per MW in 2016	3
Figure 1.4 Renewable Targets of EU Member States [1]	4
Figure 1.5 Wind Power Capacity of Leading Countries in 2016	5
Figure 1.6 Wind Power Production of Leading Countries in 2016	6
Figure 1.7 Wind Power Production of Leading Countries in 2016	7
Figure 1.8 Renewable energy share in total energy consumption by EU for 2015, 2020 targets and 2030 potential according to REmap [2]	7
Figure 1.9 Renewable energy shares for 2010, 2030 Reference Case and 2030REmap [3]	8
Figure 2.1 Damper windings in a synchronous generator [4]	13
Figure 2.2 Frequency behaviour in electric grid with the water level in a con- tainer analogy [5]	16
Figure 3.1 Variable Speed Geared Wind Turbine Model	19
Figure 3.2 Power Coefficient Variation with Tip Speed Ratio under Zero Pitch Angle	21

Figure 3.3 Power Coefficient Variation for Two Different Pitch Angle	23
Figure 3.4 Pitch Angle Control Diagram	23
Figure 3.5 Power Coefficient Varion for GE 2.75-103	24
Figure 3.6 Gearbox Modelling	25
Figure 3.7 Machine Side Control Diagram	27
Figure 3.8 Grid Side Control Diagram	28
Figure 3.9 Modified MSC for Inertial Support	30
Figure 4.1 Active Power Flow Diagram	33
Figure 4.2 Increase in the Active Power Output for Varying Wind Speeds . . .	35
Figure 4.3 Active Power Output of the Wind Turbine for Low Wind Scenario .	37
Figure 4.4 Active Power Output of the Wind Turbine for Low Wind Scenario .	37
Figure 4.5 Generator Speeds of the Wind Turbine for Low Wind Scenario . .	38
Figure 4.6 Turbine Torque, Generator Speed and Torque for 5 Seconds Sup-	
port under Low Wind Speed	39
Figure 4.7 Turbine Torque, Generator Speed and Torque for 10 Seconds Sup-	
port under Low Wind Speed	39
Figure 4.8 Turbine Torque, Generator Speed and Torque for 20 Seconds Sup-	
port under Low Wind Speed	40
Figure 4.9 DC-Link Voltage for 20 Seconds Support in Low Wind Speed . .	40
Figure 4.10 Active Power Output of the Wind Turbine for Medium Wind Scenario .	41
Figure 4.11 Generator Speed, Generator and Turbine Torques for Medium Wind Scenario for 5 Seconds Support	42

Figure 4.12 Generator Speed, Generator and Turbine Torques for Medium Wind Scenario for 10 Seconds Support	42
Figure 4.13 Generator Speed, Generator and Turbine Torques for Medium Wind Scenario for 20 Seconds Support	43
Figure 4.14 DC-Link Voltage for 20 Seconds Support in Medium Wind Speed .	43
Figure 4.15 Active Power Output of the Wind Turbine for High Wind Scenario .	44
Figure 4.16 Pitch Angle, Generator Speed, Generator and Turbine Torques for High Wind Scenario for 5 Seconds Support	45
Figure 4.17 Pitch Angle, Generator Speed, Generator and Turbine Torques for High Wind Scenario for 10 Seconds Support	46
Figure 4.18 Pitch Angle, Generator Speed, Generator and Turbine Torques for High Wind Scenario for 20 Seconds Support	46
Figure 4.19 DC-Link Voltage for 20 Seconds Support in High Wind Speed . . .	47
Figure 4.20 Probability Density Function of Measured Wind Speeds	48
Figure 4.21 Cumulative Distribution Function of Measured Wind Speeds	48
Figure 5.1 P.M.Anderson Test Case	50
Figure 5.2 Location of the Additional Load	52
Figure 5.3 Generator Frequencies for 10% Load Connection	53
Figure 5.4 Frequencies in Generator 1, Load A and Load B	53
Figure 5.5 Modified System Single Line Diagram	54
Figure 5.6 Comparison of Base Case and Modified Case Frequencies	56
Figure 5.7 Comparison of Base Case and Modified Case Frequencies	56
Figure 5.8 Comparison of Base Case and Modified Case Frequencies	57

Figure 5.9 Comparison of Base Case,Modified Case and Decommissioned
Case Frequency Responses 59

Figure 5.10 Comparison of Base Case,Modified Case and Decommissioned
Case RoCoFs 59

LIST OF ABBREVIATIONS

AC	Alternating Current
AGC	Automatic Generation Control
CDF	Cumulative Distribution Function
DC	Direct Current
DFIG	Doubly Fed Induction Generator
FSIG	Fixed Speed Induction Generator
GSC	Grid Side Converter or Controller
HCS	Hill-Climb Search
IGBT	Insulated Gate Bipolar Transistor
LSC	Line Side Converter or Controller
LVRT	Low Voltage Ride-Through
MOSFET	Metal Oxide Semiconductor Field Effect Transistor
MSC	Machine Side Converter or Controller
PDF	Probability Density Function
PI	Proportional-integral
PLL	Phase Lock Loop
PMSG	Permanent Magnet Synchronous Generator
P&O	Perturb&Observe
PSF	Power Signal Feedback
RES	Renewable Energy System
RoCoF	Rate of Change of Frequency

LIST OF SYMBOLS

C_p	Power Coefficient
λ	Pitch or Blade Angle
ω_m	Generator Speed
ω_{max}	Maximum Generator Speed
T_{Plim}	Torque Limited by Active Power of Wind Turbine
T_{Slim}	Torque Limited by Apparent Power of Wind Turbine

CHAPTER 1

INTRODUCTION

1.1 Global Renewable Energy Status

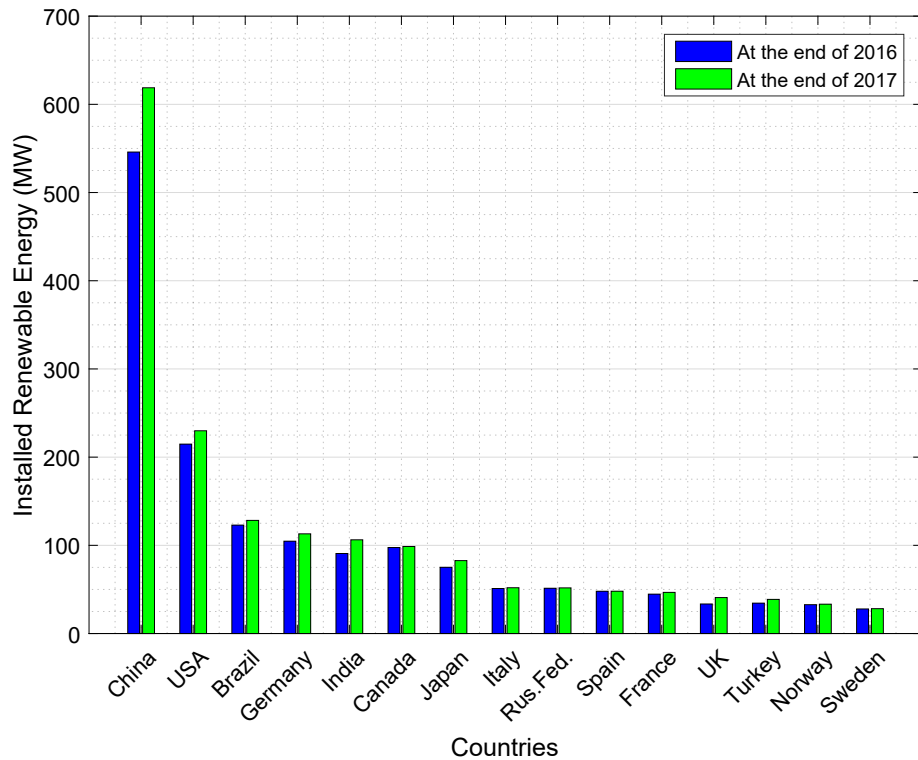


Figure 1.1: Installed Renewable Energy Capacity of Leading Countries

Renewable energy is still one of the hottest topics in the power area. The share of the renewable energy systems has been reached significant levels. At the end of 2017, the renewable power capacity has reached 2179 GW throughout the world including hydro power plants [6]. Fig. 1.1 shows the installed renewable energy capacity

for leading countries at the end of 2016 and 2017 [7], [6]. China, USA, Brazil and Germany constitutes almost half of the world total capacity. China has the biggest installed renewable capacity so far and increased its capacity by 73 GW in 2017 which is very close to the whole installed electrical power of the Turkey. This indicates the severity of the growing renewable demand.

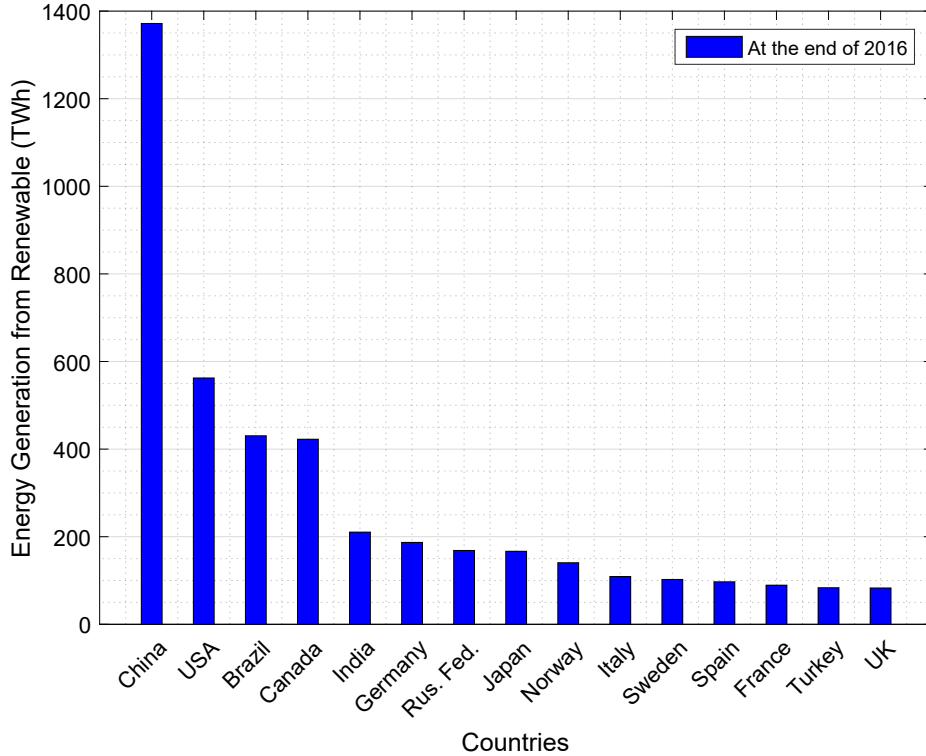


Figure 1.2: Renewable Energy Production of Leading Countries

Fig. 1.2 shows the energy production from renewable energy systems International-RenewableEnergyAgency2017. It is obvious that China, USA and Brazil produces highest amount of energy from renewable since they already have the highest installed capacity. However, India and Canada produces more energy than Germany even though Germany has more installed renewable capacity. This result is due to the fact that renewable energy production is dependent on parameters such as solar radiation and wind speed depending on the renewable source. This can be better observed in Fig. 1.3 which shows the average energy generation from per MW renewable energy sources in 2016 [7]. For a MW renewable energy system, Germany produces the lowest amount of energy meanwhile Canada and Norway produce highest amount

among these countries. Turkey has one of the lowest installed capacity and energy generation from renewable systems among the listed countries. However, it is listed in the middle of these countries due to its high potential for renewable energy systems.

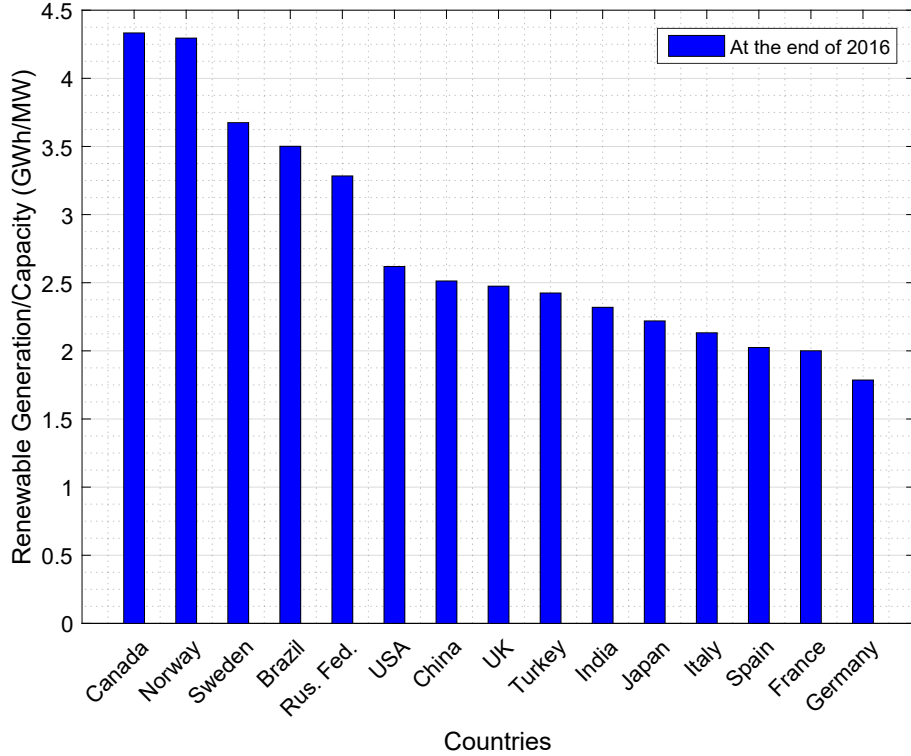


Figure 1.3: Average Renewable Energy Generation per MW in 2016

1.1.1 EU 2020 Goals

In 2008, 20 20 by 2020-Europe's Climate Change Opportunity report has been released by EU Commission and two key targets are set for 2020 [8]:

- At least 20 % reduction in greenhouse gases (GHG) by 2020
- Achieving 20% renewable energy share in energy consumption of EU by 2020

The Renewable Energy Directive is published in 23 April 2009. This directive has set national binding targets for EU countries in order to accomplish the 20% renewable

energy target for EU and 10 % target for the renewable energy usage in the transport. [9] As a result, each EU country has been determined their national action plans. In order to achieve the 20 % target, each member state determine their own targets ranging from 10% in Malta to 49% in Sweden. According to the latest release by Eurostat, renewable share of the EU in energy consumption has reached 17 % in 2016 [1]. Moreover, eleven of EU member states has already achieved their 2020 targets. Renewable shares of EU members are shown in Figure 1.4.

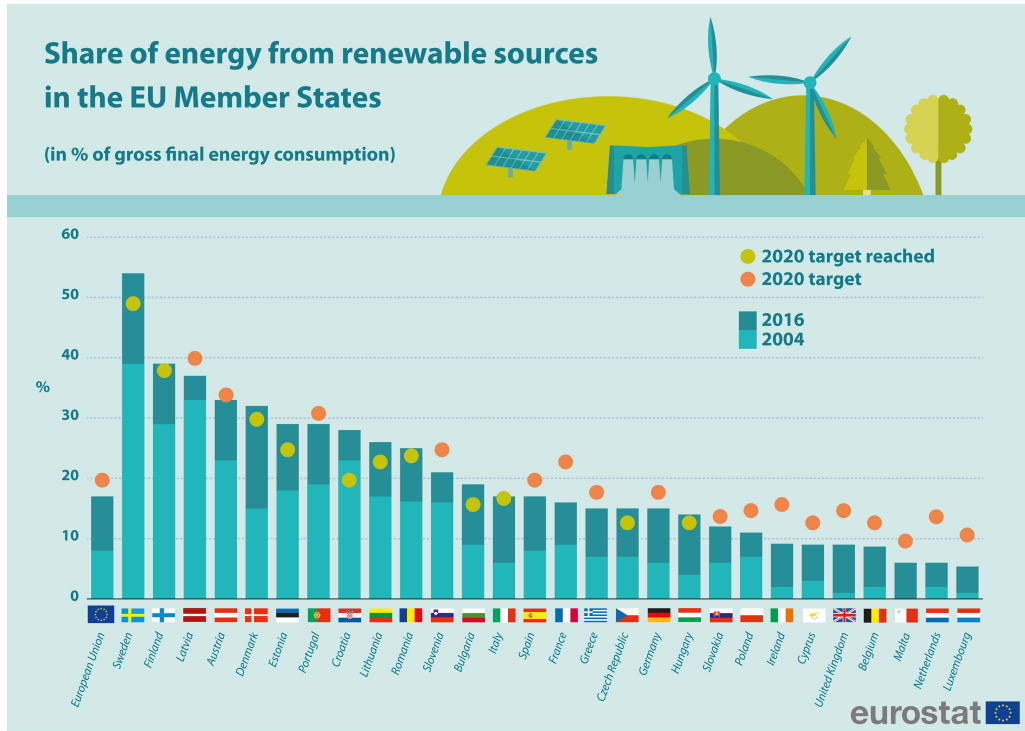


Figure 1.4: Renewable Targets of EU Member States [1]

1.1.2 Wind Energy Status

Wind power has the highest share in the installed renewable energy capacity except for hydro power. The wind power capacity at the end of 2017 has reached 514 GW worldwide [6]. The wind power capacity of the leading countries is shown in the Fig. 1.5. As in the case of total installed renewable energy capacity, China and USA have also the highest installed capacities in the wind power capacity.

The energy production from wind energy is shown in the Fig. 1.6. Even though China

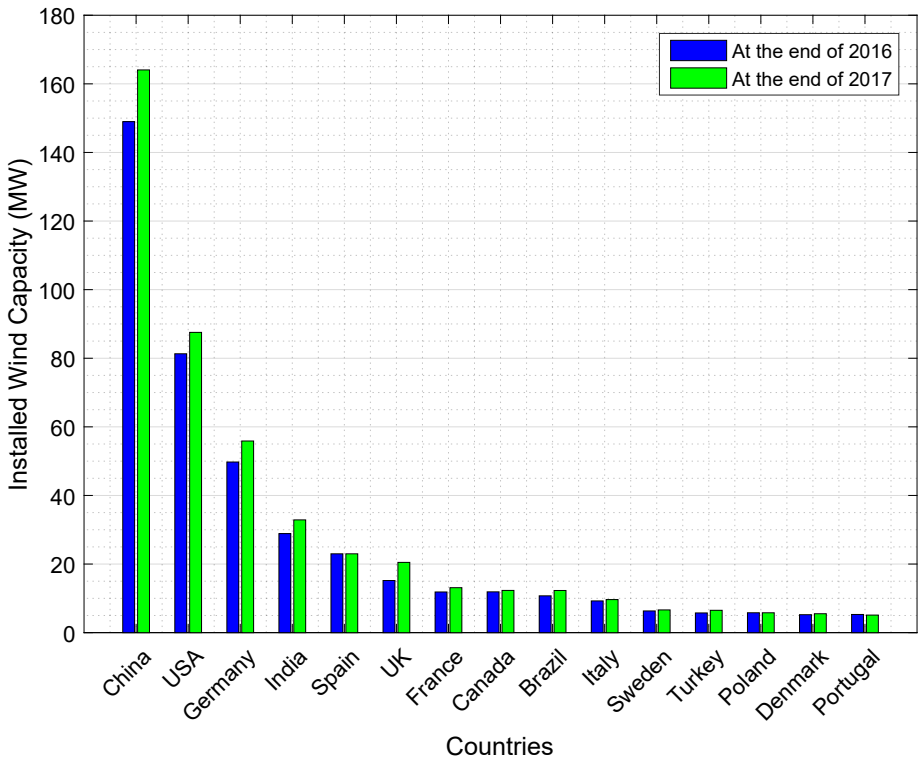


Figure 1.5: Wind Power Capacity of Leading Countries in 2016

has the highest wind power capacity, USA generates highest amount of energy from wind. The energy production per a MW wind energy system is shown in the Fig. 1.7. Denmark, UK and Sweden yield highest energy from per MW wind energy system due to its wind potential meanwhile Germany, India and China generates minimum energy.

1.2 Global Renewable Energy Future

The share of renewable energy is increasing each passing day. Today, reports arguing the possibility of even 100% renewable energy region by region is published [10]. The renewable energy reports estimate the share of renewable energy in the total energy consumption for 2030 and 2050. Figure 1.8 shows the EU renewable energy share for 2030. Moreover, the report published by IRENA (International Renewable Energy Agency) estimates the share of renewable energy in EU as 24% by 2030 which

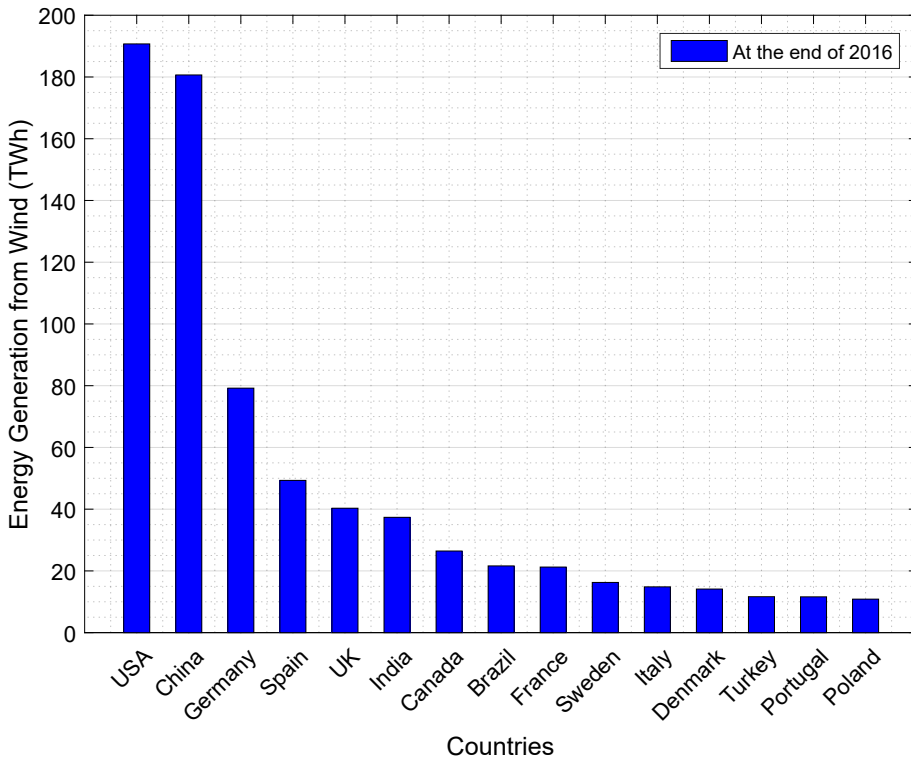


Figure 1.6: Wind Power Production of Leading Countries in 2016

is below proposed target of 27% [3].

Renewable shares of REmap countries in 2010, 2030 reference case and 2030REmap and the world average are also shown in Fig.1.9. The only country whose renewable energy decreases in the 2030 is Nigeria. The reason is that the main source of energy in Nigeria is biogas for the time being. However, the renewable share is expected to decrease dramatically as the industry switches to natural gas.

1.3 Renewable Energy Problems

It is an undeniable fact that renewable energy systems are advantageous in terms of global warming and carbon dioxide emission. Nonetheless, they also have disadvantages to the system operators due to intermittent energy generation profile. First of all, the term intermittent in the literature is related to the variable and uncontrollable nature of the renewable sources [11]. Since the source of the RES is variable, it is not

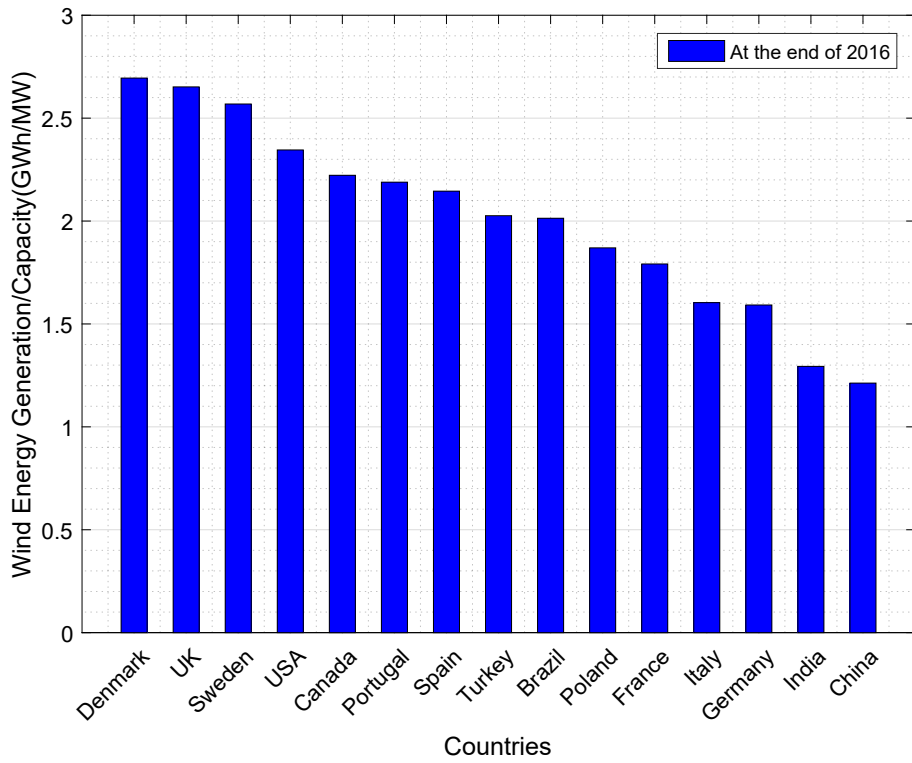


Figure 1.7: Wind Power Production of Leading Countries in 2016

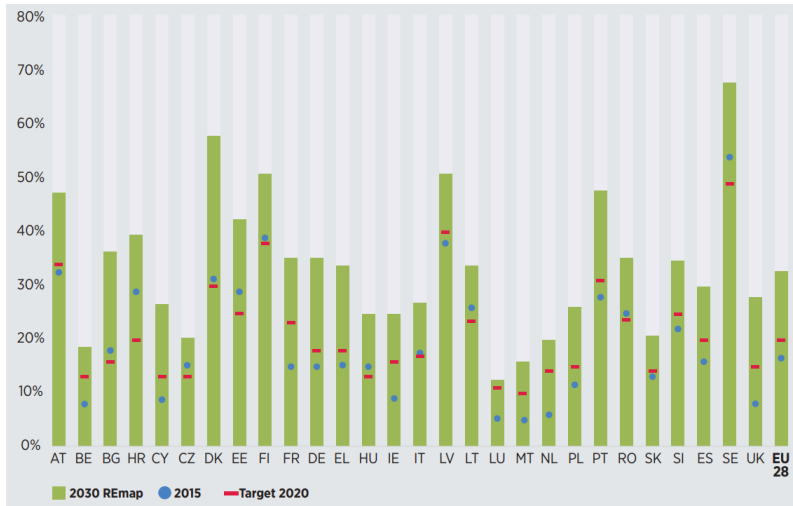


Figure 1.8: Renewable energy share in total energy consumption by EU for 2015, 2020 targets and 2030 potential according to REmap [2]

possible to adjust its output according to the demand. Therefore, the thermal plants have to be in the operation when high wind speeds and solar radiation exist. More-

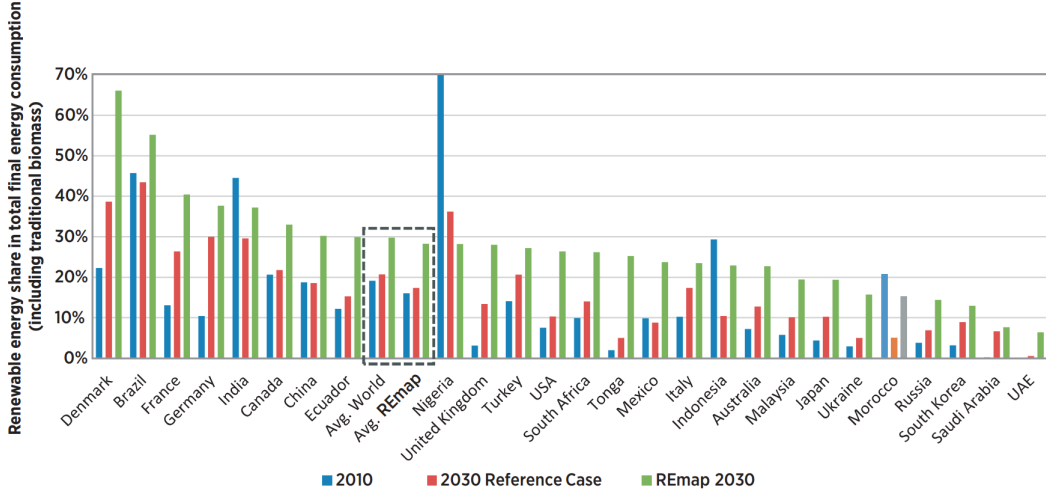


Figure 1.9: Renewable energy shares for 2010, 2030 Reference Case and 2030REmap [3]

over, the system requires additional start-ups and rise from partly loaded plants in order to balance the energy in the system because of the uncertainty of RES. These all create additional costs caused by high share of RES in the system [12]. Moreover, power grid will face with transmission system issues as overloaded transmission lines, changes on the protection and control in the distribution system, greater level of power-factor control and low voltage ride-through (LVRT) requirements when the RES share is increased in the grid [13].

Another challenge of increasing RES is the problem of power system frequency stability. Since the frequency of the power system depends on the balance between generation and consumption, grid operators are responsible for adjusting the generation in order to maintain a constant frequency. However, the renewable energy generation is strictly dependent on the renewable source i.e. solar radiation or wind speed. Therefore, renewable systems makes the system operation harder due to their intermittent and uncertain power generation profiles. Moreover, as the renewable systems with power electronics interface increase in the electricity grid, the grid equivalent inertia decreases. In [14], the reduced grid inertia due to the high DFIG wind turbine penetration is emphasized. Moreover, the results of the reduced grid inertia following a disturbance is listed as:

- increased effective aggregated angular acceleration of synchronous machines

which require high restoring forces

- high rate of change of frequency and hence, decreased frequency nadir

It should be noted that this problem is not specific to DFIG wind turbines but renewable energy systems which are connected to grid with power electronics. Conventional synchronous generators rotates with synchronous speed which is proportional to grid frequency. If the grid frequency decreases, then the synchronous speed also decreases. In this case, the generator active power is increased inherently due to kinetic energy extraction from the generator inertia. The increase in active power provides action time for primary controllers and crucial for frequency stability. Type-1 and Type-2 wind turbines are directly connected to grid. Hence, the frequency deviations affects the active power output of such wind turbines [15]. Nonetheless, active power output of renewable energy systems with power electronics such as Type-3 and 4 wind turbines and photovoltaic systems is not affected from the grid frequency deviations. Therefore, these system have no contribution to the grid inertia whether the system includes inertia or not. Hence, the aggravated grid inertia is reduced with the penetration of RES. The comparison for different type of generators is made in [16] and listed in Table 1.1.

Type of the generator	Inertial Response Behaviour
Conventional Synchronous Generator	++
Fixed Speed Induction Generator (FSIG)	+
Doubly Fed Induction Generator (DFIG)	-
Variable Speed Wind Turbine Generator (Connected with Full Scale Power Electronics)	None

Table 1.1: Comparison of Different Type of Generators for Inertial Response Behaviour

Another reason for the decrease in the grid inertia is the de-commitment or dispatch of the conventional sources due to economic concerns. Since the renewable energy has the lowest cost for energy production, it preferred instead of conventional generators. As a result, conventional generators are dispatched to a lower generation profile or taken-off from operation.

Note that grid inertia is directly related to the amount of load in the system in addition to the share of RES. Therefore, the amount of online generator fluctuates within time. Hence, the scenario in which the system has low demand and also high renewable generation is the most critical one since the lowest grid inertia will be faced in the network.

1.4 Literature Review

Studies regarding inertial support date back to early 2000s. In the study [17], the effect of the increasing wind energy penetration has been investigated. The study concludes that increasing share of wind energy increases the primary reserve requirement for the successful grid operation. The increased frequency deviations, especially in light load conditions (high wind generation with low consumption scenario) can be mitigated in the system as long as the wind generation provides inertia support. Study in [18] states that DFIG wind turbines are de-coupled from power system resulting in no contribution to system inertia. A supplementary loop is proposed for reinstating the machine inertia. Moreover, in [19], performance of the supplementary control loop is evaluated with the comparison of the inertial support of a fixed-speed wind turbine. The proposed control loop has been validated in [20] and compared with the droop control in [21].

It is an undeniable fact that renewable energy systems are the most economical way of producing electrical energy due to absence of any fuel cost. Therefore, they are to be operated in their rated power. However, they have to curtail their power in order to leave a margin for droop control. Droop control by wind energy is also studied in the literature. In [15], the inertial support of different type of wind turbines is compared. It is concluded that the Type-4 wind turbines are able to perform better performance for inertial support due to the power electronics interface. Moreover, combination of inertial support and droop control produces better results in these wind turbines.

1.5 Thesis Motivation

The frequency of the electric grid depends on the balance between generation and consumption. Grid operators are responsible for maintaining this balance so that frequency of the grid is maintained between allowed dead-band. In order to achieve this purpose, power generation is adjusted according to the consumption value. However, the balance between supply and demand might be disturbed with unintentional generator trip or instant load connections. Grid frequency decreases such instants until the generation is increased to arrest the frequency. Inertia of the electric grid provides additional power from the stored kinetic energy and avoid the system frequency from decreasing down very fast. That is called as inertial support and it is very important for power system frequency stability.

Although renewable energy systems are beneficial for environmental concerns and lower energy cost, higher renewable penetration also brings operational challenges for system operators. One of the most important problem that comes with renewable energy is the power system frequency stability. With the high renewable penetration, grid aggravated inertia decreases. As a result, grid frequency deviates steeper for disturbances. To avoid steeper frequency declines in the grid, all generation technologies should provide inertial support for the frequency disturbances.

Wind energy systems, especially variable speed wind turbines with full scale power electronics are the most promising renewable energy systems that can contribute to grid frequency stability thanks to their high inertia in their blades and generator and also their back-to-back converters that give ability to control its active power. Therefore, wind energy conversion systems are required to participate in ancillary services for frequency stability in order to reach a stable power system network in the upcoming future.

1.6 Thesis Outline

This thesis study focuses on the inertial support capability of variable speed the wind turbines. The thesis starts with a brief summary of the renewable energy status in Chapter 1. By reviewing the share of the renewable energy systems and the targets

for upcoming future highlight the importance of the frequency stability studies. In the Chapter 2, the frequency concept in power systems is extensively described. Since the conventional power generation units are replaced or preferred over renewable energy sources, the electricity grid is facing with frequency stability issues due to the absence of inertia-less units. Therefore, the behaviour of old-fashion power plants are described under frequency disturbances. Since the existing variable speed wind turbines require modification in order to integrate to electricity grid, detailed modelling of these wind turbines is presented in Chapter 3. The modification in order to mimic synchronous generator behaviour is also described in this chapter. In this way, wind turbines with full scale power electronics are able to adjust their active output power according to the frequency deviations in the point of interconnection.

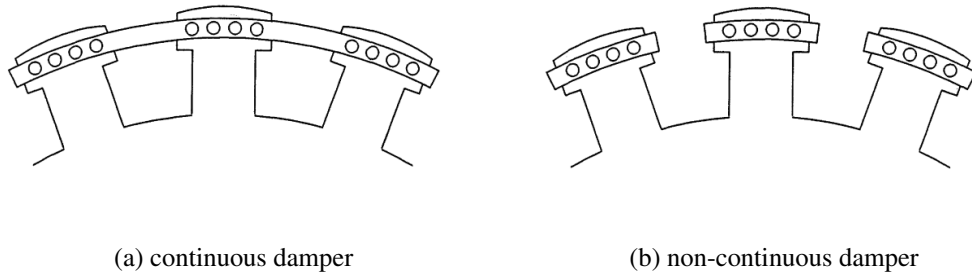
The limits of the active power increase is investigated in Chapter 4. The ability of increasing its active power output is already presented in the literature. However, the amount of additional power based on the wind speed is studied. Moreover, the real wind speed measurements are utilized in order to find the probability of such increased power is detected. It is to note that the amount of the inertial support in this chapter is not dependent on the rate of change of frequency. This chapter only explores the capability of the wind turbine for a defined wind speed. Inertial support based on frequency deviations as in the case of conventional synchronous generators are studied in the Chapter 5 on a P.M. Anderson 9 bus test case. Different inertia constants are emulated on a wind farm to see the improvements on the power system frequency stability. Test case is modified with different combinations in which the system is penetrated with wind farm with/without generator decommission are studied in this chapter. The conclusion drawn in this thesis is presented in the Chapter blah.

CHAPTER 2

POWER SYSTEM FREQUENCY STABILITY

2.1 Synchronous Generator and Synchronous Speed

Synchronous machines produce torque only in synchronous speed. This is why they are equipped with damper windings which are basically induction machine windings. If the frequency of grid changes, damper windings create a torque which creates a force to synchronize the speed to the grid frequency. Two type of damper windings are given in Fig. 2.1.



(a) continuous damper

(b) non-continuous damper

Figure 2.1: Damper windings in a synchronous generator [4]

The synchronous machines keep their operation in the synchronous speed thanks to the damper windings in the rotor. Relation between grid frequency and the synchronous speed is given in Eq. (2.1) in terms of rpm. [4]. This equation can be better observed in Eq (2.3).

$$n_s = \frac{120f}{p_f} \quad (2.1)$$

$$n_s = \frac{60}{2\pi} \omega_{syn} \quad (2.2)$$

$$\omega_{syn} = \frac{4\pi f}{p_f} \quad (2.3)$$

where n_s is the synchronous speed in rpm, f is the grid frequency in Hz, p_f is the number of poles of the generator and ω_{syn} is the synchronous angular speed in rad/s.

2.2 Swing Equation

Speed in synchronous machines changes according to the net torque acting on the rotor. Therefore, the speed is maintained constant unless there is no difference between mechanical and electromechanical torque. The equation of motion is given in Eq. (2.4) where J is aggravated moment of inertia of the generator and the turbine in kgm^2 , T_m and T_e are mechanical and electromechanical torques in Nm .

$$J \frac{d\omega_m}{dt} = T_m - T_e = T_a \quad (2.4)$$

In power system network, the power ratings of the generators and corresponding moment of inertia values varies. Hence, it is more convenient to use inertia constant, H whose unit is seconds and varies between 2 and 9 [4]. Inertia constant is defined as the ratio of kinetic energy stored in the inertia to the power rating of the generator as in Eq. (2.5) where ω_{0m} denotes the rated angular velocity of generator in rad/s and S_{base} is the rated apparent power in VA.

$$H = \frac{\frac{1}{2} J \omega_{0m}^2}{S_{base}} \quad (2.5)$$

Substituting Eq. (2.5) into Eq. (2.4) and replacing units to per-unit quantities yield the relation of frequency with power and inertia constant as in Eq. (2.10).

$$J = \frac{2H}{\omega_{0m}^2} S_{base} \quad (2.6)$$

$$\frac{2H}{\omega_{0m}^2} S_{base} \frac{d\omega_m}{dt} = T_m - T_e \quad (2.7)$$

$$\frac{2H}{\omega_{0m}^2} S_{base} \omega_m \frac{d\omega_m}{dt} = P_m - P_e \quad (2.8)$$

$$2H \frac{\omega_m}{\omega_{0m}} \frac{d(\omega_m/\omega_{0m})}{dt} = \frac{P_m - P_e}{S_{base}} \quad (2.9)$$

$$2H \overline{\omega_m} \frac{d\overline{\omega_m}}{dt} = \overline{P_m} - \overline{P_e} \quad (2.10)$$

2.3 Frequency in Power Systems

The frequency in a power system is related to the speed of the synchronous generators and changes according to the swing equation. The frequency of each generator is not the same in the network since each generator does not have the same speed. There are always fluctuations in the power system. However, the network can be assumed as a single generating unit by neglecting this assumption. The swing equation basically investigates the relation between mechanical and electromechanical powers and the rate of change of angular speed of a generator. Therefore, the speed of a generator remains constant if the mechanical and electromechanical powers are equal.

If the electricity grid is considered as a single generator, the inertia of the equivalent generator is aggregated from each generator in the network. In this case, average frequency in the network can be found as in Eq. (2.11)

$$2H_{sys} \overline{f_{sys}} \frac{d\overline{f_{sys}}}{dt} = \overline{P_m} - \overline{P_e} \quad (2.11)$$

where P_m is the aggregated mechanical input power of the generators meanwhile P_e is the aggregated electromechanical output power. In other words, the system frequency depends on the balance between generation and consumption. Note that generation means the input mechanical power of the generators.

The behaviour of the frequency in electric grid is depicted in Fig. 2.2. As it can be seen from the water level in a container analogy, the frequency of the system is dependent on the in-flow and the out-flow. Therefore, in the electricity grid, frequency increases as the aggregated input power is higher than the aggregated output power. Note that, the direction of the frequency is dictated by this balance. Having a constant

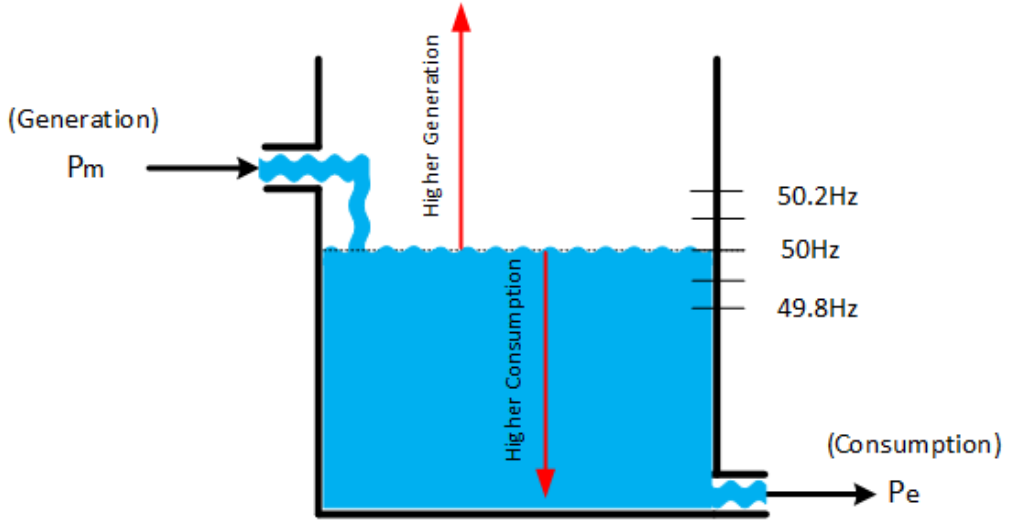


Figure 2.2: Frequency behaviour in electric grid with the water level in a container analogy [5]

49.8Hz frequency does not mean that consumption is higher than generation. If the frequency is constant, then the input mechanical power is equal to output power.

2.3.1 Primary Frequency Control

Having a constant frequency is one of the most important responsibilities of a system operator. In order to have a constant frequency, supply is being adjusted according to the demand continuously. By doing so, the system frequency varies between a band-gap. The variation depends on the disturbances which are generally a sudden generation outage or instant load connection. The size of the disturbance determines the severity of the frequency change and there are three main mechanisms to arrest the frequency changes in the system.

Following generator outage or sudden load connection event, frequency starts decreasing. The slope of the frequency is dependent on the severity of the event by means of power and the available inertia of the power system. Such frequency disturbance requires increased input power. However, the increase in the input mechanical power should be activated very fast and should be automated. This responsibility is assigned to generating units with primary control. The active power generation of these units is increased or decreased by the governor depending on the network frequency di-

rection. Note that each generator in the power system does not necessarily perform primary control function. In this case, their active power generation is independent from the network frequency. Hence, the decrease in the frequency is arrested by the primary frequency control. The primary controllers act during a few seconds following a disturbance. They keep their operation up to 30 minutes.

2.3.2 Secondary and Tertiary Control

The frequency is recovered back to nominal value with the Secondary Frequency Control action. This controller might be a single or multiple centres that monitor the frequency and adjust the generation accordingly. They are also called as Automatic Generation Control (AGC) systems and their action takes a few minutes. The final frequency control mechanism is the Tertiary Frequency Control. If the frequency is not recovered back to nominal value with the secondary controllers, tertiary frequency controllers manually activates the load shedding which is an undesired situation by the network operator. However, it is an emergency case which might result in black-out and requires immediate action.

CHAPTER 3

WIND TURBINE MODELLING

3.1 Variable Speed PMSG Wind Turbines

The share of variable speed PMSG wind turbines is increasing worldwide due to the high efficiency and torque density. This type of wind turbines are equipped with full-scale power electronics which enable the turbine to have wide speed range. Even though the price of the permanent magnet fluctuates with time, the reliability and high efficiency of this type of turbine increase its share in the market.

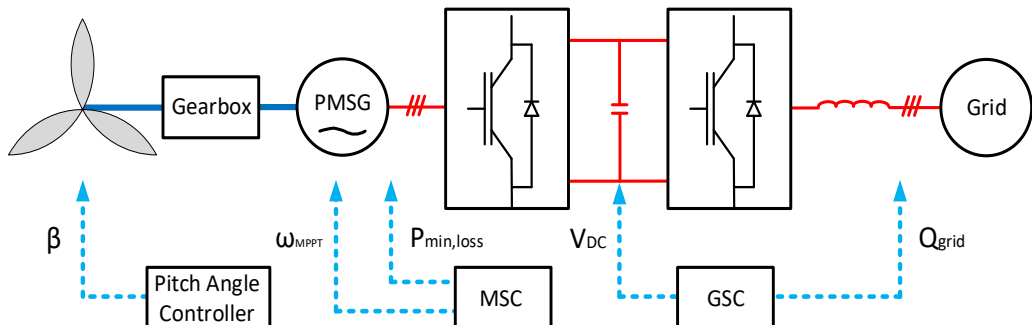


Figure 3.1: Variable Speed Geared Wind Turbine Model

Fig. 3.1 shows the modelling of variable speed PMSG wind turbine. The source of the power in these systems is the wind itself. The power is captured from the wind with the help of three-blade turbine. Three-blade turbine is the aerodynamic part of the system and it applies a aerodynamic torque to gearbox. In fact, this torque is the source of the movement and dictates the direction of the movement. Aerodynamic torque is applied to gearbox which establishes the connection between turbine and generator. In variable speed wind turbines, stator of the PMSG is not directly connected to grid. A back-to-back converter is used between generator and the elec-

trical grid to ensure that the turbine speed is independent from the grid frequency. The converter which is connected to PMSG is called Machine Side Converter (MSC) meanwhile the one connected to grid is called Grid Side Converter(GSC). Moreover, GSC is connected to grid with a filter in order to filter out high frequency currents due to switching action.

3.1.1 Aerodynamic Model

Aerodynamic model is the sub-model that captures power from the wind. The output of this block is the aerodynamic torque that rotates the turbine. However, the wind speed is not the only input. Turbine speed and pitch angle are also the inputs of the system since they affect the mechanical power that is captured from the wind.

The aerodynamic power of wind is given in Eq. (3.1) where ρ_{air} is air density in kg/cm^3 , R is the blade radius in m abd v_{wind} is the wind speed in m/s . Note that this is the available power of the air that is striking the turbine swept area and it is not possible to extract that amount of energy. Otherwise, the air would be standstill behind the wind turbine [22].

$$P_{WIND} = 0.5\rho_{air}\pi R^2 v_{WIND}^3 \quad (3.1)$$

The wind turbine captures a fraction of the available wind power that is denominated as power coefficient C_p . Therefore, turbine power captured from wind can be found with the Eq. (3.2).

$$P_{TUR} = C_p P_{wind} \quad (3.2)$$

Power coefficient determines the amount of power to be captured from wind and it is a non-linear function of the tip speed ratio, λ and pitch angle, β . Tip speed ratio is a parameter proportional with turbine speed. It can be defined as the ratio of the speed in the turbine tip to the wind speed as in the Eq. (3.3). Power coefficient for a specific tip speed ratio and pitch angle can be found with the Eq. (3.4) and (3.5) where c_1 is 0.5176, c_2 is 116, c_3 is 0.4, c_4 is 5, c_5 is 21 and c_6 is 0.0068 [23].

$$\lambda = \frac{\omega_{tur}R}{v_{wind}} \quad (3.3)$$

$$C_p(\lambda, \beta) = c_1(c_2/\lambda_i - c_3\beta - c_4)e^{-c_5/\lambda_i} + c_6\lambda \quad (3.4)$$

$$\frac{1}{\lambda_i} = \frac{1}{\lambda + 0.08\beta} - \frac{0.035}{\beta^3 + 1} \quad (3.5)$$

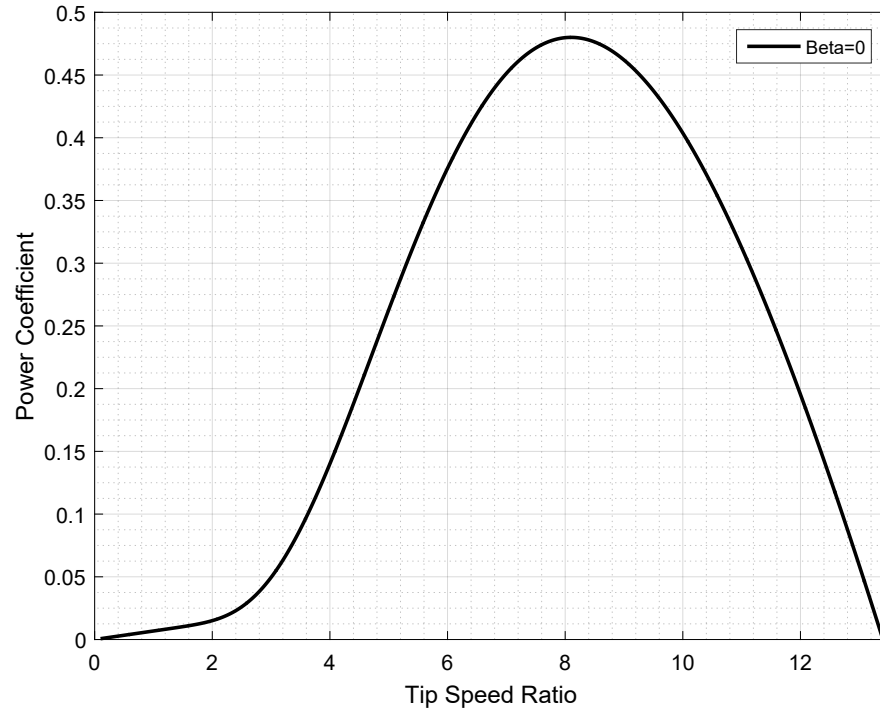


Figure 3.2: Power Coefficient Variation with Tip Speed Ratio under Zero Pitch Angle

Variation of power coefficient C_p is given in Fig. 3.2 for varying tip speed ratio. For the zero pitch angle, power coefficient has the maximum value of 0.48 for the tip speed ratio of 8.1. In order to ensure that the maximum of wind power is extracted, wind turbine should rotate a speed that gives the optimum tip speed ratio. This is ensured by the Maximum Power Point Tracking (MPPT) algorithms.

3.1.1.1 Maximum Power Point Tracking Algorithms

In the literature, numerous different methods are presented in order to operate in the Maximum Power Point. Perturb&Observe (P&O) is the most common MPPT method

in the literature [24], [25]. The methods simply creates a perturbation in the generator speed. The change in the generator speed creates also change in the active power output. If the power is increased with this perturbation, the generator speed is again perturbed in the same direction until a decrease in the active power is observed. This method is the simplest method and does not require any calculation or wind speed measurement. However, the algorithm creates oscillations in the generator speed and active power. This method is also called as Hill-Climb Search (HCS) method in the literature.

Another MPPT algorithm is the wind speed measurement method [26], [27]. If the wind speed is estimated accurately, the optimal generator speed can be calculated. However, wind speed estimation is complicated and increases the cost. One other commonly used MPPT algorithm is the power-signal feedback (PSF) control [27], [24], [28]. This method requires maximum power curve of the wind turbine based on the experimental results. A look-up table is constructed with obtained wind turbine speed and active output power values. However, using generator speed and active power measurements is the main drawback of this algorithm. Finally, there are numerous number of much complex MPPT algorithms based on fuzzy-logic [29] or neural-network [30]. However, these MPPT algorithms are out of scope of this thesis. Therefore, optimal generator speed is provided in this study according to the wind speed.

3.1.1.2 Pitch Angle Control

According to Eq. (3.1), wind power increases with the cube of the wind speed. Hence, wind power increases dramatically for the high wind speeds. In order to decrease power, pitch angle i.e. blade angle is increased. Since the power coefficient, C_p is a function of the pitch angle, β , wind power can be curtailed with increased blade angle. Variation of power coefficient for two different pitch angle is shown in Fig. 3.3. Increasing pitch angle by 1.176° decreases power coefficient by 10%.

As long as wind power is below the rated power, the wind turbine is operated in MPPT speed. This is ensured by obtaining optimal tip speed ratio. This means that for zero pitch angle, MPPT speed is increased linearly with wind speed. Before

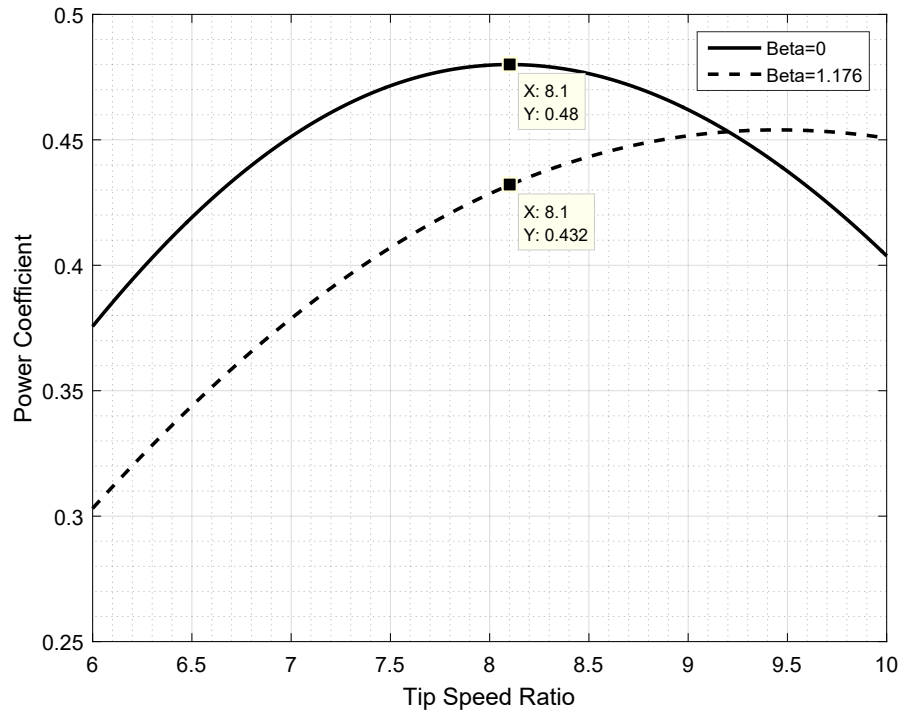


Figure 3.3: Power Coefficient Variation for Two Different Pitch Angle

reaching rated power, MPPT speed might reach maximum generator speed. In this case, wind turbine reference speed will be the maximum generator speed. However, turbine speed cannot be decreased down to reference speed when the torque limit is reached. Hence, the pitch angle should be increased to regulate the turbine speed. Pitch angle controller is depicted in Fig. 3.4. Note that the pitch angle is increased when the speed exceeds maximum generator speed. Otherwise, the pitch angle kept as zero.

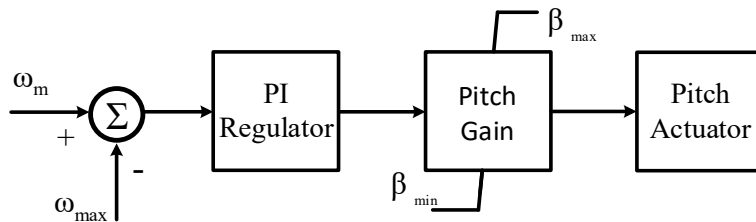


Figure 3.4: Pitch Angle Control Diagram

It is to note that the pitch angle controller takes action as soon as the maximum generator speed is exceeded. Therefore, wind turbine operation deviates from optimal

tip speed ratio. This can also be observed from the variation of power coefficient, C_p with the wind speed for the wind turbine GE 2.75-103 used in this study. Variation of the C_p is shown in Fig. 3.5.

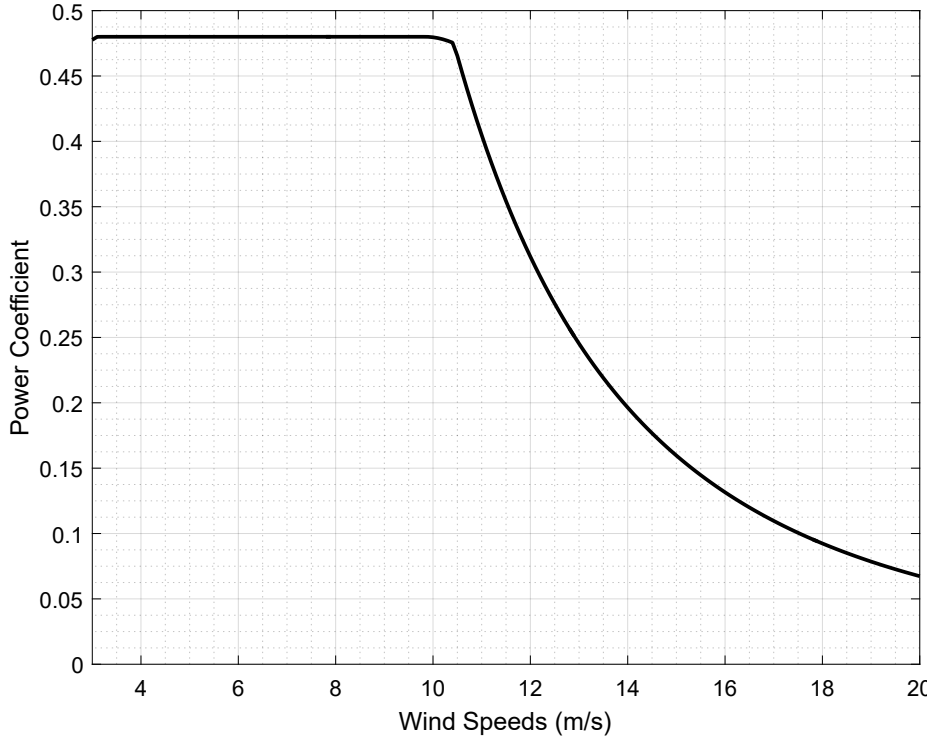


Figure 3.5: Power Coefficient Varion for GE 2.75-103

3.1.2 Gearbox

Variable speed PMSG wind turbines have a gearbox between turbine and generator except for direct-drive wind turbines. The gearbox increases angular speed and decreases the torque in the generator side. By decreasing the rated torque, generator size and cost can be reduced since the generator size is almost proportional to rated torque due to constant shear stress [31]. Moreover, turbine speed is increased to the allowable speed range of the generator which is generally much higher than that of wind turbines. Otherwise, generator should have high pole numbers.

A gearbox model is depicted in Fig. 3.6. They are mainly used for speed and torque

conversion. It should be noted that the gearboxes are not full efficient systems. Therefore, the output torque of the gearbox would be lower than the ratio of input torque to gearbox conversion ratio. Direct-drive systems are based on the elimination of the gearbox systems by direct connection between turbine and generator in order to increase efficiency and reliability [32]. In this study, gearbox system is modelled with 100% efficiency.



Figure 3.6: Gearbox Modelling

3.1.3 Permanent Magnet Synchronous Generator

PMSGs are generally preferred over electrically excited synchronous generators due to high efficiency due to the fact that absence of electrical excitation on the rotor decreases losses. Besides, slip ring is not needed in the generator which also decrease the maintenance. Dynamical equations of the salient pole PMSG are projected on a reference frame which rotates synchronously with magnet flux and given in Eq. (3.6) and (3.7) where R_1 is stator resistance in Ω , L_{sd} and L_{sq} are d and q axis inductances in H , i_{ad} and i_{aq} are d and q axis currents in A , ω is the electrical angular frequency in rad/s ψ_f is magnet flux linkage in Vs [22].

$$v_{1d} = R_1 i_{ad} + L_{sd} \frac{di_{ad}}{dt} - L_{sq} \omega i_{sq} \quad (3.6)$$

$$v_{1q} = R_1 i_{aq} + L_{sq} \frac{di_{aq}}{dt} + L_{sd} \omega i_{sd} + \omega \psi_f \quad (3.7)$$

Another important PMSG parameter is the power in dq frame. The power expression is given in Eq. (3.8). The electromechanical torque can be found by the relation between power and angular speed. The torque expression is also given in Eq. (3.9)

where p is the number of pole pair.

$$P_{elm} = \frac{3}{2}\omega i_{aq}(\psi_f + i_{ad}(L_{sq} - L_{sd})) \quad (3.8)$$

$$T_e = \frac{P_{elm}}{w_m} = \frac{P_{elm}}{w/p} = \frac{3}{2}pi_{aq}(\psi_f + i_{ad}(L_{sq} - L_{sd})) \quad (3.9)$$

Given equations are defined for salient pole machines. If the cylindrical rotor machine is used, the torque equation reduces to the Equation 3.10.

$$T_e = \frac{3}{2}pi_{aq}\psi_f \quad (3.10)$$

3.1.4 Machine Side Converter

Variable speed wind turbines are equipped with the Back-to-Back converters in order to decouple grid frequency and the turbine speed. This gives wind turbine degree of freedom for the rotational speed. In this way, turbine is able to capture the maximum available power from wind. Machine Side Converter (MSC) i.e. Generator Side Converter is the converter that is connected between generator and DC-bus. The three phase generator output AC voltage is converted to DC voltage. Conversion from AC to DC can be achieved by three-arm full bridge converters. This converter can be equipped with uncontrolled, semi-controlled and fully-controlled switches. Fully-controlled switches such as MOSFET, IGBT are commonly used in the industry and gives two control parameters to the user.

Voltages and currents are generally transformed into synchronously rotating reference frame or also called dq frame. Since the frame is rotating in synchronous speed, three-phase phasors are transformed to DC quantities. Therefore, its control becomes easier [33]. Proportional-integral (PI) controllers are associated with the dq control structure due to their satisfactory behaviour interaction to DC variables [34]. Hence, the control in the back-to-back converter is achieved with PI controllers in the dq frame.

The control diagram of the MSC is depicted in Fig. 3.7 according to the study in [35]. In dq frame, it is possible to control two parameters. One of these parameters is the d-axis current. It can be set zero in order to decrease the stator copper losses. The

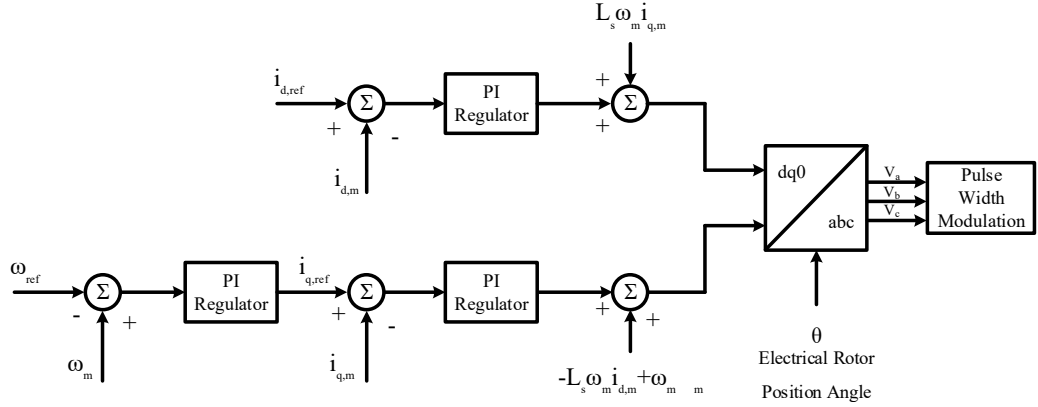


Figure 3.7: Machine Side Control Diagram

other parameter is the q-axis current that is proportional to the electromagnetic torque as it can be observed in the Eq. (3.10). However, q-axis current or torque is controlled in order to regulate the turbine speed. Therefore, turbine speed is adjusted such that the turbine will capture maximum available power in the wind.

3.1.5 Grid Side Converter

Grid Side Converter (GSC) or Line Side Converter (LSC) is the converter that is connected between DC-link capacitance and grid. GSC works as an inverter that injects current synchronous with grid voltage. Currents and voltages are transformed into synchronously rotating frame that is aligned with the grid voltage. Therefore, d-axis current determines the amount of current which is in phase with the grid voltage meanwhile q-axis current determines amount of current that is out of phase with the grid voltage. In other words, injecting d-axis current injects active power to grid meantime q-axis current injects reactive power to grid.

The responsibility of the GSC is regulating DC voltage and the reactive power injected to grid. The control diagram of the GSC is given in Fig. 3.8. As seen from the figure, DC-bus voltage is regulated by controlling the d axis current. If the DC-bus voltage increases above the reference value, d-axis current reference is increased. As a result, active power increases. Increased active power also decreases the DC-bus voltage level. Reference value of the q-axis current is set to zero in normal operation, consequently unity power factor. For Low Voltage Ride-Through studies, q-axis

current is determined according to the reactive power value requirement. [36]

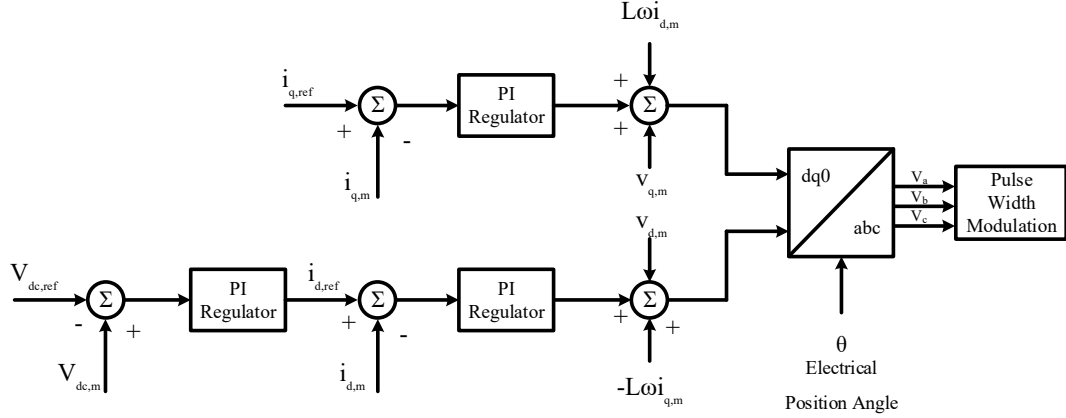


Figure 3.8: Grid Side Control Diagram

GSC is connected to grid through an filter. Therefore, the output voltage of the converter is not equal to the that of grid. The relation between converter voltage, grid voltage and current is derived through Eq. (3.11) to (3.17) where v_c is the converter voltage, v_g is the grid voltage and i_g is the grid current measured in the grid side. As it is observed in Eq (3.16) and (3.17), converter side voltage includes same axis grid voltage and a term proportional to cross axis current which is called cross-coupled term. Therefore, the outputs of the inner PI regulators are compensated and forwarded to Pulse Width Modulation after transformation to three-phase voltages.

$$\bar{v}_c = v_{dc} + jv_{qc} \quad (3.11)$$

$$\bar{v}_g = v_{dg} + jv_{qg} \quad (3.12)$$

$$\bar{i}_g = i_{dg} + ji_{qg} \quad (3.13)$$

$$\bar{v}_c = \bar{v}_g + \bar{i}_g j\omega L \quad (3.14)$$

$$v_{dc} + jv_{qc} = v_{dg} + jv_{qg} + j\omega L(i_{dg} + ji_{qg}) \quad (3.15)$$

$$v_{dc} = v_{dg} - \omega L i_{qg} \quad (3.16)$$

$$v_{qc} = v_{qg} + \omega L i_{dg} \quad (3.17)$$

3.2 Synthetic Inertia Implementation

As explained in Chapter 2 Section 2.2, synchronous generators changes its speed according to the balance between input mechanical and electromechanical powers. The inverse case is also true. In other words, if the frequency changes, the electromechanical power of the generators also change. Synthetic inertia is the method that implements this behaviour on the renewable energy systems. It is possible to change the active power output of the wind turbines if these are connected to grid with full scale power electronics. The increase in the active power should be proportional to change of frequency and the inertia of the renewable energy system. Even though renewable energy system does not have inertia, inertial support with desired inertia constant can be implemented in the system as long as a stored energy exists in the system.

In order to implement synthetic inertia in the system, a relation between frequency and active power of the wind turbine should be constructed. Wind turbine in this study is variable speed wind turbine with full scale power electronics. The speed of the turbine is controlled by MSC such that active power is adjusted. Inertial support modification is depicted in Fig. 3.9. The new value of the active power is determined according to the swing equation. However, the wind turbine in this study is operated with a reference speed rather than a reference power. Therefore, the assigned power value should be used in order to yield the q-axis current reference value. Reference q-axis current is derived between the Eq. (3.18) to Eq. (3.21).

$$P_{new} = (1 + \Delta P)P_{pre} \quad (3.18)$$

$$T_{new}\omega_m = (1 + \Delta P)T_{pre}\omega_{pre} \quad (3.19)$$

$$\frac{3}{2}p\psi_f i_{q,new}\omega_m = (1 + \Delta P)\frac{3}{2}p\psi_f i_{q,pre}\omega_{pre} \quad (3.20)$$

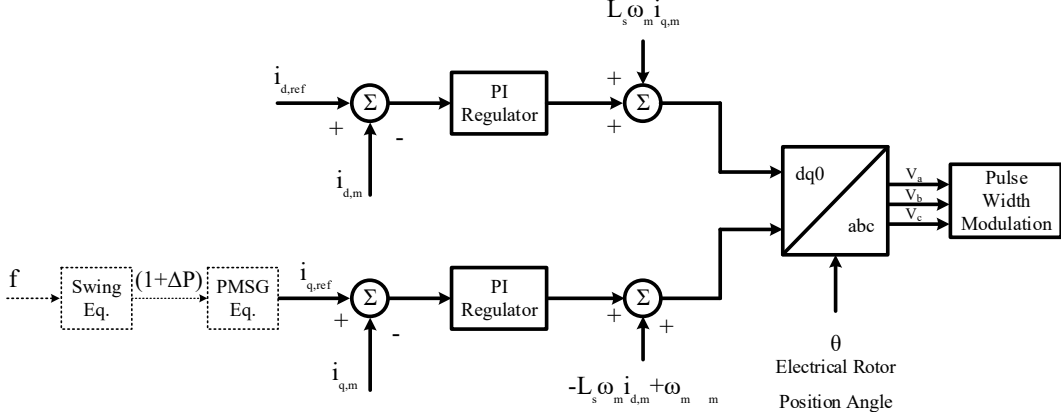


Figure 3.9: Modified MSC for Inertial Support

$$i_{q,ref} = i_{q,new} = (1 + \Delta P) \frac{i_{q,pre}\omega_{pre}}{\omega_m} \quad (3.21)$$

3.2.1 Synthetic Inertia Activation Schemes

Another issue about inertial support is the time instant to trigger synthetic inertia. In the literature, continuous operation, under-frequency trigger and maximum-frequency gradient are discussed [37]. It is obvious that continuous operation would create oscillations in active power output due to the continuous deviations in grid frequency. This is an unrealistic operation and is used for comparison purposes.

Second activation method is the under-frequency trigger which is the activation when the frequency decreases below a threshold value. It can be used for capturing the time instant for the inertial support. However, power grid might be in a stable point even if the frequency is 49.8Hz. Therefore, this method would be unsuccessful depending on the disturbance event.

Third activation scheme is the maximum-frequency gradient trigger. It uses a controller that is very similar to RoCoF relays and tracks the frequency gradient. Once the frequency gradient is below a threshold value, the synthetic inertia is activated. Since the severity of frequency disturbance event is related to the RoCoF, this activation scheme is the most remarkable scheme [37]. In this study, maximum-frequency gradient is used with a threshold value of 0.1Hz/s.

3.2.2 Source of the Inertial Support

Renewable energy systems convert the energy captured from wind or sun to the electrical energy. Hence, the renewable energy systems cannot determine the amount of power in contrast the conventional systems. A thermal power plant, for instance, adjusts its power output as desired. However, the source of power in renewable energy is constant for a definite wind speed or solar radiation. This is why a spare energy is required in order to change the power output.

Energy stored in DC bus capacitance is the only stored energy in PV systems. The amount of energy is given in Eq. (3.22) and negligible for inertial support studies. In the wind energy systems, there exists huge amount of kinetic energy in wind turbine generator and blades in addition to electrostatic energy. The kinetic energy expression is given in Eq. (3.23). Note that J_{total} is the equivalent inertia in the generator side and ω_m is the speed of the generator.

$$E_{electrostatic} = \frac{1}{2}C_{DC}V_{DC}^2 \quad (3.22)$$

$$E_{kinetic} = \frac{1}{2}J_{total}\omega_m^2 \quad (3.23)$$

Note that the amount of kinetic energy is dependent on the generator speed. Therefore, the stored energy in wind turbines changes according to the generator speed. Moreover, it can also be concluded that the energy is dependent on the wind speed. However, the generator speed is kept constant if the wind speed increases above the rated wind speed.

To illustrate the situation better, the electrostatic energy stored in DC bus and kinetic energy in turbine equivalent inertia are compared for GE2.75-103 wind turbine. The wind turbine has a DC bus capacitance of $27mF$ and $1200V$ DC link voltage. The corresponding electrostatic energy is calculated in Eq. (3.24). The generator speed of the corresponding generator is between $550rpm$ and $1735rpm$. The total turbine inertia is $1058.2kgm^2$ in generator side. The minimum and maximum kinetic energy values are calculated in Eq. (3.25) and (3.26). These values are found out to be 90 and 900 times of the electrostatic energy stored in DC bus capacitance.

$$E_{DC-Link} = \frac{1}{2}27(10^{-3})1200^2 = 19.44kJ \quad (3.24)$$

$$E_{kinetic,min} = \frac{1}{2}(1058.2)57.6^2 = 1755.17kJ \quad (3.25)$$

$$E_{kinetic,max} = \frac{1}{2}(1058.2)181.7^2 = 17466.02kJ \quad (3.26)$$

CHAPTER 4

INVESTIGATION OF INERTIAL SUPPORT PRACTICAL LIMITS

4.1 Inertial Support Limits

The source of power in a wind turbine is the aerodynamic wind power, P_{wind} which is constant for a constant wind speed, pitch angle and generator speed. In the steady state, this power is transferred through MSC as P_{gen} . If there is a difference between P_{wind} and P_{gen} , the difference is either stored in or extracted from the turbine and generator inertia as in the form of kinetic energy. Grid power, P_{grid} is received from MSC and injected grid. The difference between P_{gen} and P_{grid} is stored in or extracted from DC-bus capacitance. The active power flow diagram is depicted in Fig. 4.1. As mentioned in Chapter 3, stored energy exists in turbine and generator inertia and DC-bus capacitance. However, it is also stated that the E_{kin} is much larger than E_{DC} even in the lowest generator speed. Therefore, the source of the inertial support studies is the kinetic energy stored in the inertia.

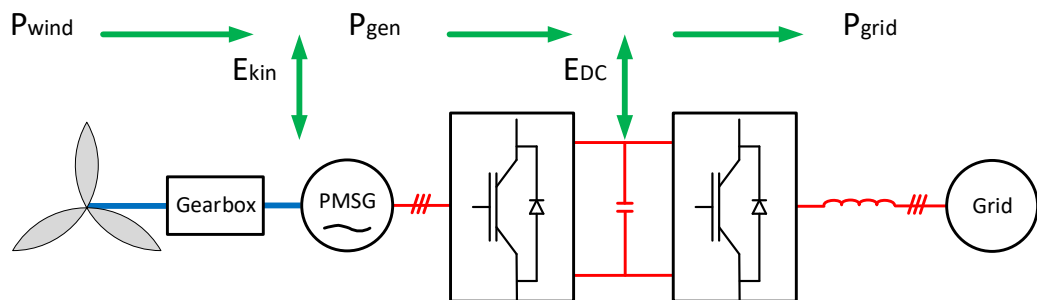


Figure 4.1: Active Power Flow Diagram

Wind turbine active power can be increased by increasing the generator power P_{gen} . This can be achieved by adjusting the generator torque since the active power is pro-

portional to electromagnetic torque. However, the active power is also dependent on the generator rotational speed as in Eq. (4.1). The active power can be increased by increasing the turbine torque but the increase is limited by the generator speed. Therefore, the active power increase is also dependent on the wind speed which determines MPPT speed in the steady state.

$$P_{gen} = T_e \omega_m \quad (4.1)$$

Note that the source of the additional power is the kinetic energy stored in the turbine equivalent inertia. Therefore, as soon as the power is increased, the turbine and generator speeds start decreasing. Therefore, the electromagnetic torque should be increased to keep the generator power constant. The time duration that generator power is increased and the initial generator speed will determine the final generator speed as in the Eq. (4.2).

$$\int_{t_i}^{t_f} P_{wind} - \int_{t_i}^{t_f} P_{gen} = \Delta E_{kin} = \frac{1}{2} J_{tur} (\omega_f^2 - \omega_i^2) \quad (4.2)$$

As seen from the Eq. (4.1), the generator power is the multiplication of generator torque and speed. In the high speeds, the generator speed ω_m , cannot be controlled with only the generator torque but also with the pitch angle. In this way, the rated power is not exceeded as in the Eq. (4.3) by maintaining the maximum generator speed and maximum generator torque. However, general practice is employing higher power rating converter than generator active power rating in the variable speed wind turbines. Therefore, higher limit torque can be used in such wind turbine applications by considering the apparent power of the back-to-back converters. Therefore, the maximum power for a wind speed can be defined as in Eq. (4.4).

$$P_{rated} = T_{P-lim} \omega_{max} \quad (4.3)$$

$$P_{max} = T_{S-lim} \omega_{max} \quad (4.4)$$

It is obvious that the maximum available active power is dependent on the generator speed, hence, the wind speed for the corresponding operation time. This is why the amount of the active power increase also depends on the wind speed. By considering the MPPT speed operation in GE 2.75-103 model wind turbine, the maximum increase in the active power is shown in Fig. 4.2. The wind turbine can increase its

active power by the lowest amount when the wind speed is high. Since the turbine output power is already close to converter maximum power rating, the increase in the active power is much lower than that of low wind speed operations. It is observed that the wind turbine output power can be increased by 0.45 pu when the wind speed is between 5m/s and 8m/s.

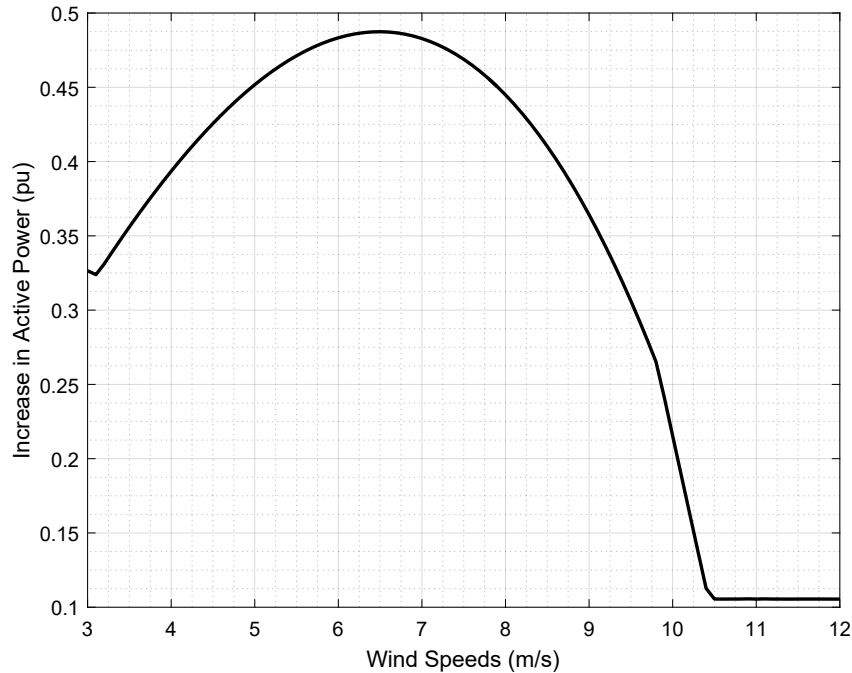


Figure 4.2: Increase in the Active Power Output for Varying Wind Speeds

It is already stated that power system frequency is a function of input mechanical sources of conventional synchronous generators and the output active powers. Therefore, frequency disturbances occur due to the imbalance between these. Since the aim of providing inertial support in the form of fast increased active power is to arrest the frequency decline, the increase in the output power is much more important than the total active output power.

4.2 Inertial Support Under Different Wind Speeds

Active power of the wind turbines is determined by parameters such as wind speed, pitch angle and turbine speed. Therefore, combination of these parameters have im-

portance for a possible inertial support. In other words, wind turbine under high wind scenario has different potential than that under low wind scenario. Likewise, the resultant states of wind turbines for inertial support would be much different. In this chapter, the effect of wind speeds will be investigated for inertial support. Active power of wind turbines will be increased by different percentages. The change in generator speed, turbine and generator torques, DC-link voltage and pitch angle, if any, will be observed. Wind turbine used in this study is GE 2.75-103 model, variable speed PMSG.

4.2.1 Low Wind Scenario

The minimum speed of the wind turbine in this scenario is 550 rpm in the high speed side. Wind speed that will capture the maximum power from wind in this generator speed is found out to be 3.12m/s. In this scenario, the kinetic energy stored in the turbine inertia is minimum and calculated in Chapter 4 in Eq. (3.25). This scenario investigates the case where the least amount of kinetic energy exists in the turbine equivalent inertia.

4.2.1.1 Active Power Limit in Low Wind Scenario

The electricity grid in the upcoming future might require sudden active power release from wind farms for short time durations. Therefore, it is important to observe the maximum achievable power for inertial support studies. The equation Eq. (4.4) implies that wind turbine in the low wind speed scenario cannot reach rated active power since the generator speed is much lower than the maximum generator speed. However, the electromagnetic torque in steady state is much lower than the limit torque, T_{S-lim} . Therefore, the wind turbine in low speed scenario has the potential for increasing its active power to a significant value. Fig. 4.3 shows the increase of active power to maximum value. The increase is obtained by ensuring the limit torque, T_{S-lim} . However, since the generator speed is decreasing, the active power is also decreasing.

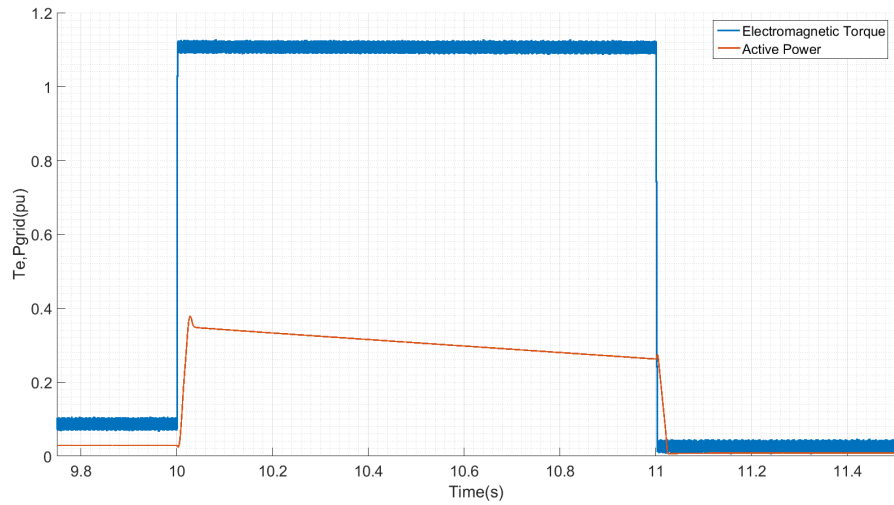


Figure 4.3: Active Power Output of the Wind Turbine for Low Wind Scenario

4.2.1.2 Active Power in Low Wind Scenario

The active power of the wind turbine is increased 10% for three different time intervals as 5, 10 and 20 seconds. The active power output of the wind turbine is given in Fig. 4.4. It is observed that turbine power decreases below the nominal value after the support period in order to recover the generator speed. Another observation is the fact that higher support time creates higher dip in the active power in the speed recovery period.

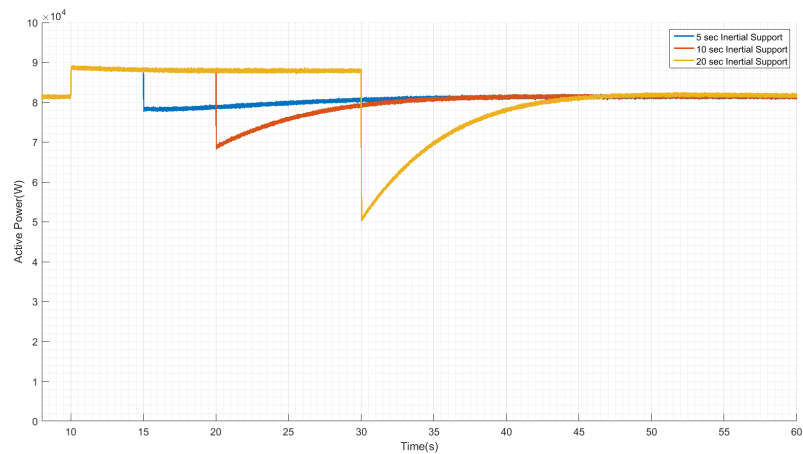


Figure 4.4: Active Power Output of the Wind Turbine for Low Wind Scenario

The source of the increased active power in this study is the kinetic energy in the turbine inertia. Therefore, additional active power is extracted from this energy causing a decrease in the wind turbine generator. Generator speed decreases continuously until the support is ended. The generator speeds are shown in Fig. 4.5 for three support times.

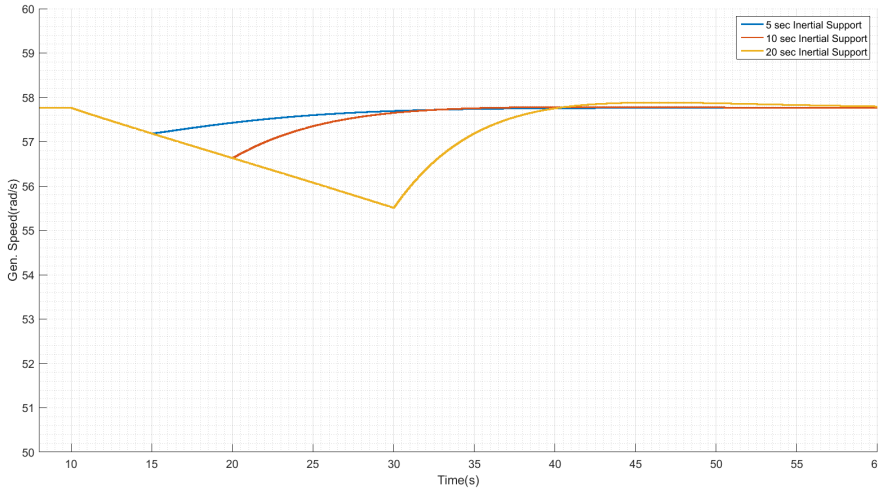


Figure 4.5: Generator Speeds of the Wind Turbine for Low Wind Scenario

The decrease in the generator speed is obtained with an increase in the generator torque. The turbine torque, generator torque and generator speed for 5 seconds support is given in Fig. 4.6. The generator torque is increased at $t=10s$ for a time duration of 5 seconds. Turbine torque increases slightly with decreasing speed. However, the increase in the turbine torque is negligible when it is compared to the increase in generator torque as shown in zoomed graph. Therefore, the turbine torque is assumed to be constant for the support period. Turbine and generator torques for the 10 and 20 seconds cases are also shown in Fig. 4.7 and Fig. 4.8. Another important criteria on inertial support studies is the DC-Link voltage. When the active power is increased, increased amount of active power is transferred from MSC to GSC. Increased active power should be injected to grid without causing excessive voltage rise on the DC-bus. Note that the voltage rise in the very first seconds in inertial support activation is same for all three support cases. However, the voltage drop will be highest in the 20 seconds case. DC-link voltage for 20 seconds support case is given in Fig. 4.9. The rise on DC-bus voltage can be considered as negligible meanwhile the

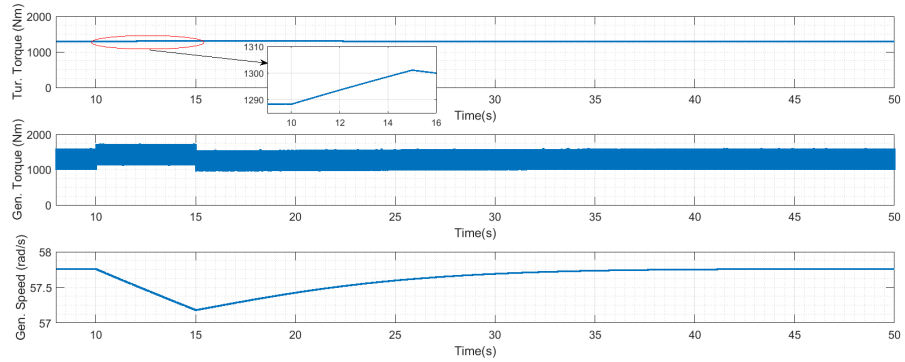


Figure 4.6: Turbine Torque, Generator Speed and Torque for 5 Seconds Support under Low Wind Speed

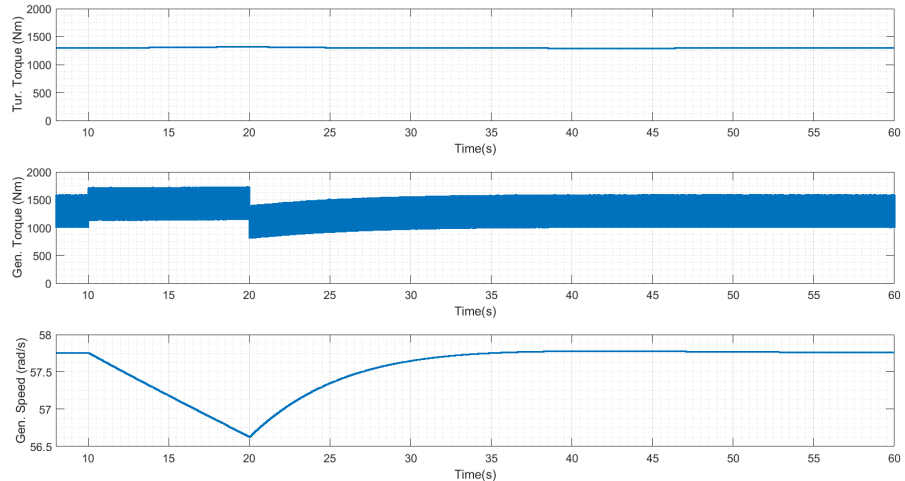


Figure 4.7: Turbine Torque, Generator Speed and Torque for 10 Seconds Support under Low Wind Speed

voltage drops to 0.9995 pu in 20 seconds support case.

4.2.2 Medium Wind Scenario

In the medium wind scenario, wind turbine operated in the middle of the generator speed range. The wind speed is selected as 6m/s in this scenario.

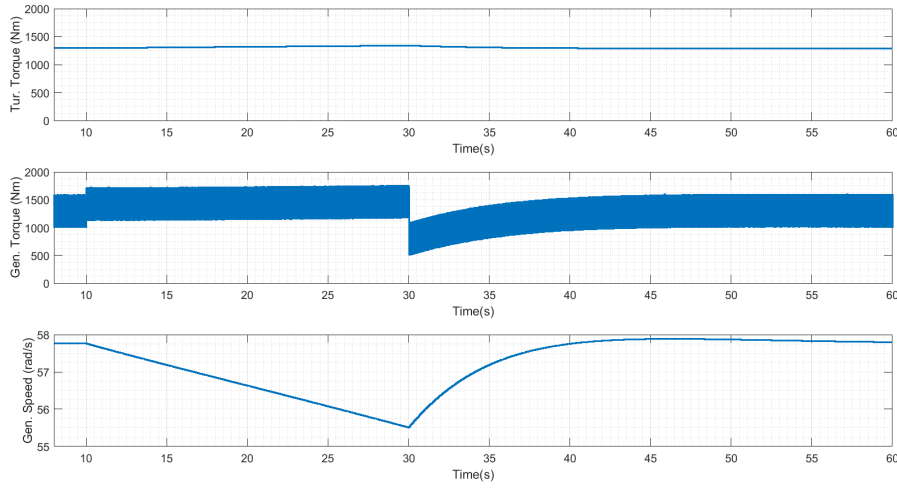


Figure 4.8: Turbine Torque, Generator Speed and Torque for 20 Seconds Support under Low Wind Speed

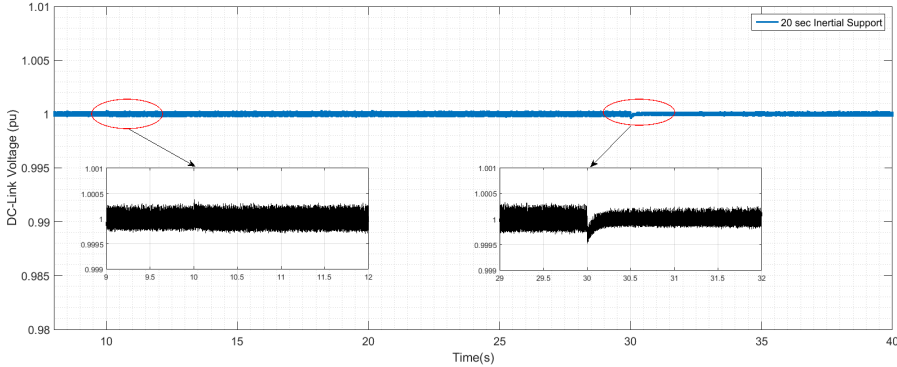


Figure 4.9: DC-Link Voltage for 20 Seconds Support in Low Wind Speed

4.2.2.1 Active Power in Medium Wind Scenario

The active power of the wind turbine is increased by 10% to provide an inertial support and it is shown in Fig. 4.10. The recovery period of shortest support case is much more smoother than the longer ones. When the support time is increased, active power of the wind turbine is almost halved that might cause also problems in frequency stability of the power systems.

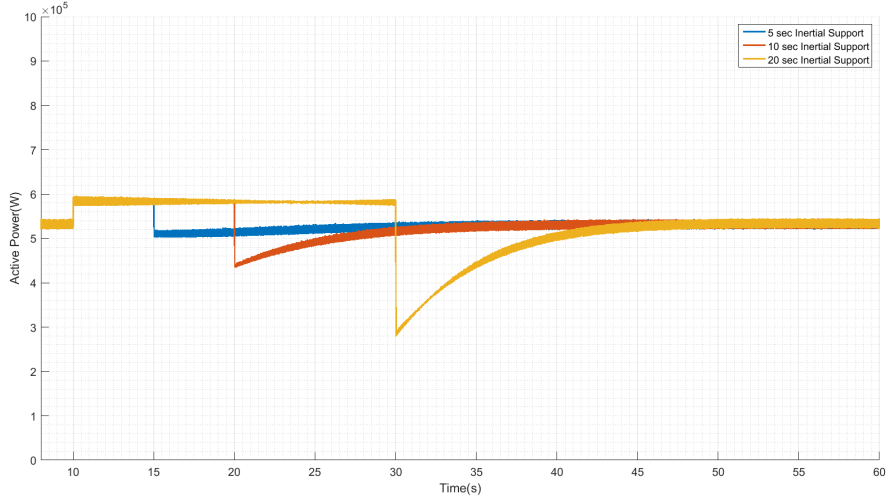


Figure 4.10: Active Power Output of the Wind Turbine for Medium Wind Scenario

4.2.2.2 Generator Speed, Turbine and Generator Torques in Medium Wind Scenario

In medium wind scenario, higher support time causes decreased active power after the support is ended. The reason is the lower speed value obtained with higher support time. Generator torque is decreased much higher for this case in order to recover the speed.

The generator speed, turbine and generator torques are shown in Fig. 4.11, Fig. 4.12 and Fig. 4.13. This can be better observed in Fig. 4.13 when the support is ended time at 30 seconds. The negative jump in generator torque creates a negative jump in the active power of the wind turbine since the transferred power is the multiplication of generator torque and generator speed.

4.2.2.3 DC-Link Voltage in Medium Wind Scenario

The variation of DC-bus voltage with inertial support is shown in Fig. 4.14. The support is activated in time 10 seconds. The rise on the DC-bus voltage is negligible as in the case of low wind scenario. However, the voltage drop at the end of support is much more significant than that of low wind scenario.

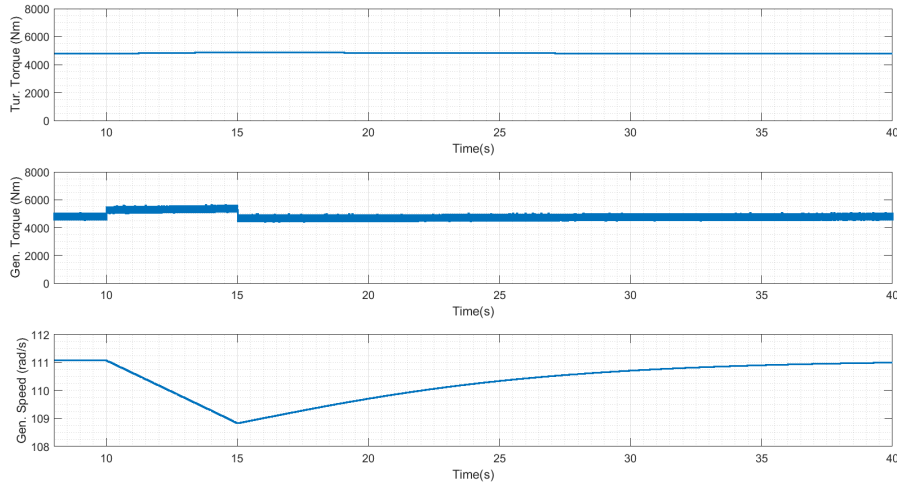


Figure 4.11: Generator Speed, Generator and Turbine Torques for Medium Wind Scenario for 5 Seconds Support

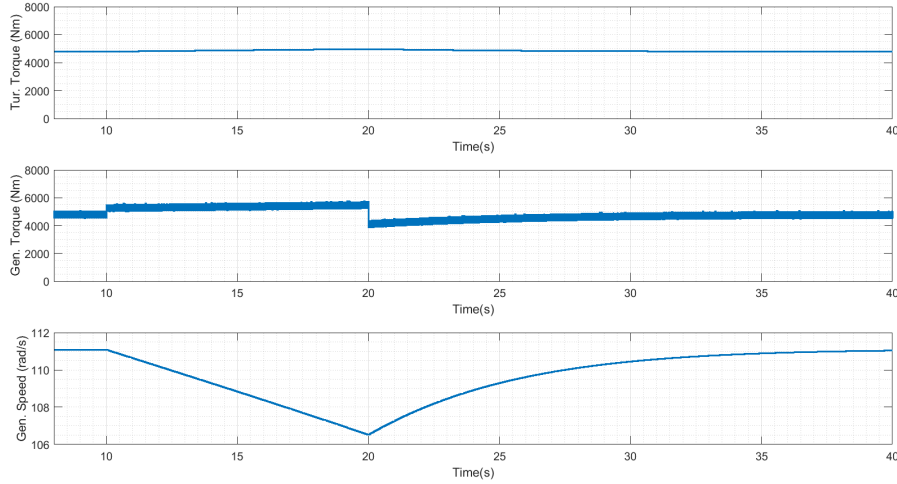


Figure 4.12: Generator Speed, Generator and Turbine Torques for Medium Wind Scenario for 10 Seconds Support

4.2.3 High Wind Scenario

In this section, wind turbine operation with high wind speed is investigated. In the high speed operation, the wind turbine injects its maximum power to grid. However, the generator reference speed is the maximum wind speed. Therefore, wind turbine

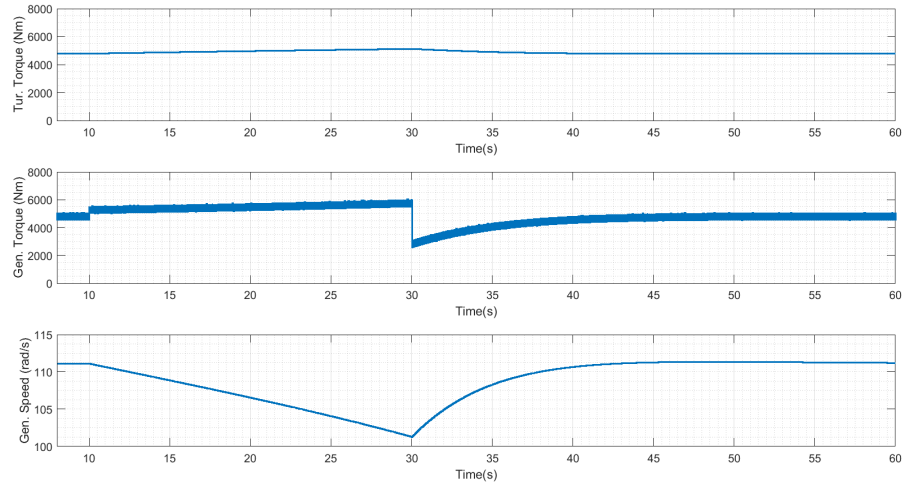


Figure 4.13: Generator Speed, Generator and Turbine Torques for Medium Wind Scenario for 20 Seconds Support

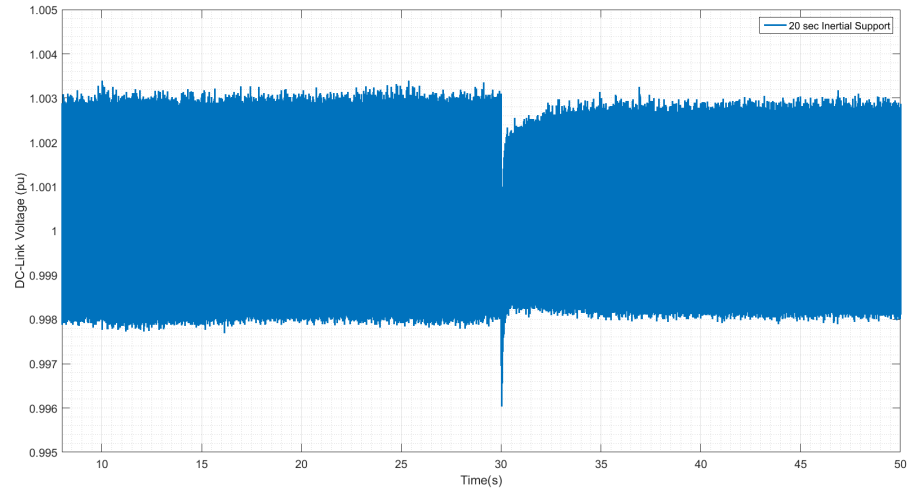


Figure 4.14: DC-Link Voltage for 20 Seconds Support in Medium Wind Speed

operation is from MPPT operation. Another difference in this section is the pitch angle that curtail wind power and ensure that the generator speed is kept at its maximum. The wind speed in this scenario is selected as 11.4m/s.

4.2.3.1 Active Power in High Wind Scenario

Wind turbines are able to provide inertial support in high wind speed as long as converter power rating is higher than the wind turbine power rating. The wind turbine investigated throughout the study has a converter rating of 3.04MVA meanwhile turbine power rating of 2.75MW. Therefore, active power output can be increased up to 3.04MW during support interval. Otherwise, wind turbine cannot provide inertial support for high wind speeds. The active power of the wind turbine is increased by 10% with three different time intervals. The active powers are shown in Fig. 4.15.

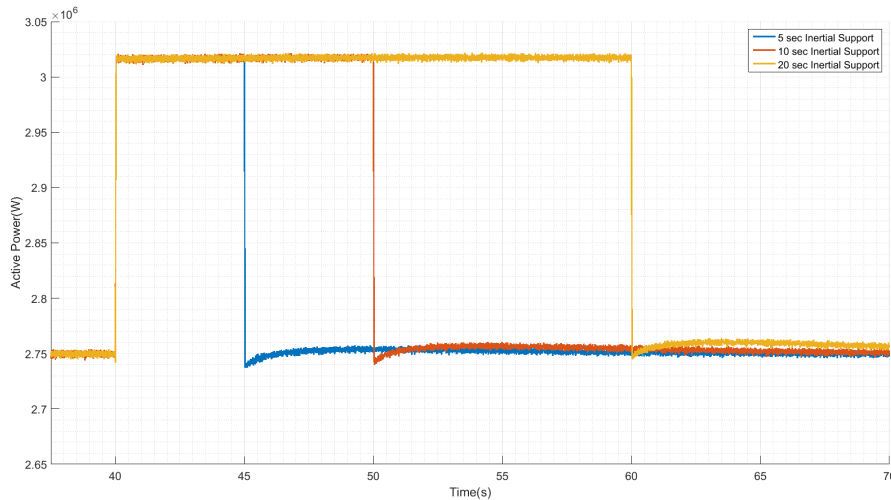


Figure 4.15: Active Power Output of the Wind Turbine for High Wind Scenario

An interesting observation in high wind scenario is that there is no speed recovery process. As soon as the speed is decreased, the pitch controller decreases the blade angle which causes an increase in turbine torque. Therefore, in this case, turbine power decreases back to normal rather than a lower power value as in the other scenarios.

4.2.3.2 Generator Speed, Turbine and Generator Torques in High Wind Scenario

In the high wind case, the generator torque hits the limit defined for normal operating conditions. This is why generator speed is regulated with the help of blade angle.

Therefore, pitch angle is also important in this section. Generator speed, turbine and generator torques as well as pitch angle for 5, 10 and 20 seconds support cases are shown in Fig. 4.16, Fig. 4.17 and Fig. 4.18. Generator speed starts decreasing when the generator torque is increased. However, the pitch controller decreases the blade angle since the generator speed is below the maximum speed. Therefore, the generator speed rises when the pitch angle is decreased. Note that pitch servo acts slower than the generator torque increase time. This is why the generator speed decreases until the pitch angle is decreased. Generator speed might not be disturbed if the pitch controller is able act fast enough.

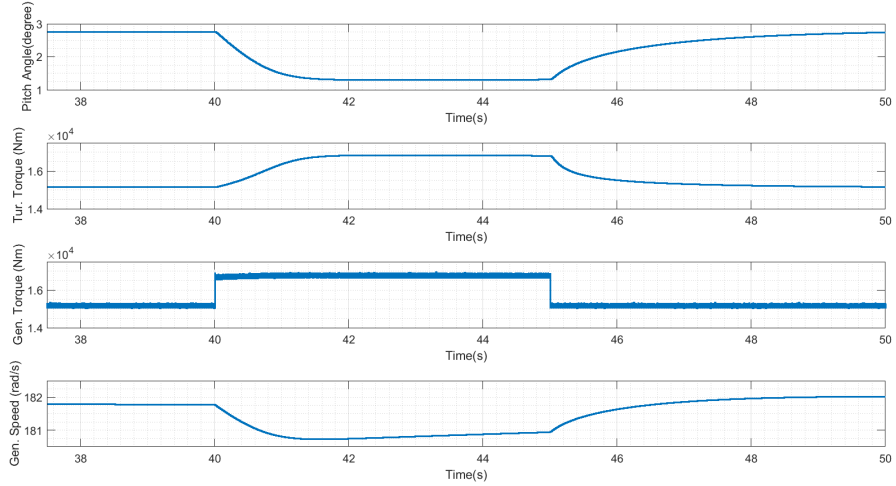


Figure 4.16: Pitch Angle, Generator Speed, Generator and Turbine Torques for High Wind Scenario for 5 Seconds Support

In high wind scenario, generator speed rises towards the maximum generator speed thanks to the decrease in blade angle. If the support time is increased, the generator speed will reach the maximum speed, and will stay constant with a new pitch angle.

4.2.3.3 DC-Link Voltage in High Wind Scenario

The DC-bus voltage is not affected from inertial support on low speed scenario. However, the nominal power and additional power in low speed case is much smaller than that of high wind scenario. The effect of inertial support in high wind case is shown in Fig. 4.19. Nonetheless, the DC-bus voltage is between the range of 0.996 and 1.004

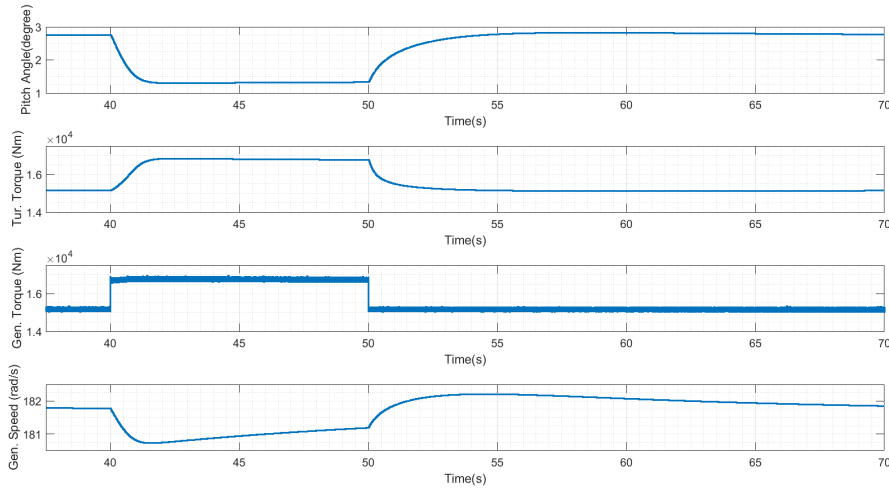


Figure 4.17: Pitch Angle, Generator Speed, Generator and Turbine Torques for High Wind Scenario for 10 Seconds Support

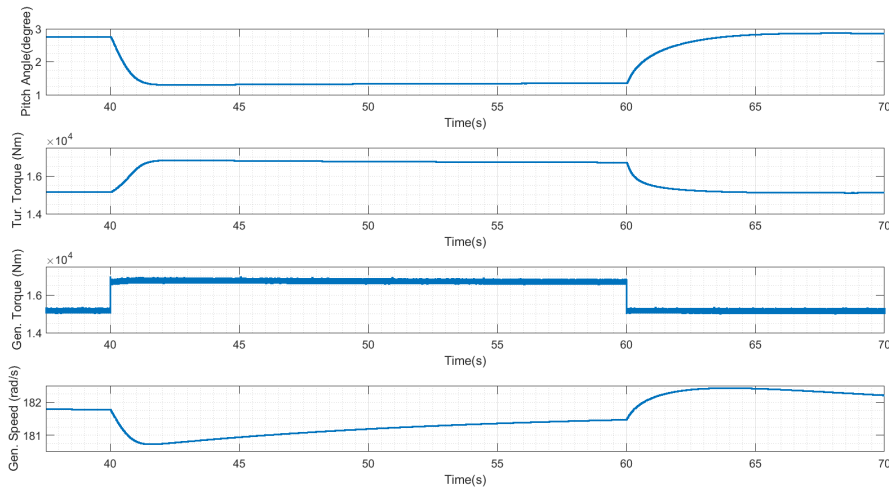


Figure 4.18: Pitch Angle, Generator Speed, Generator and Turbine Torques for High Wind Scenario for 20 Seconds Support

pu in high wind scenario. Note that wind turbines encounter such variations in the DC-bus voltage when the wind speed changes during daily operation.

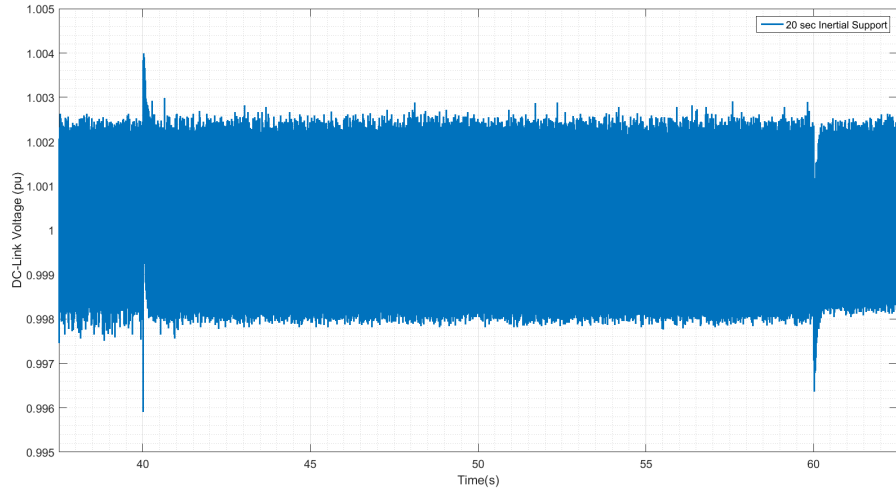


Figure 4.19: DC-Link Voltage for 20 Seconds Support in High Wind Speed

4.3 Probabilistic Approach for Different Wind Speeds

In the Section 4.1, the inertial support limits are investigated for different wind speeds. It is stated that the wind turbines can increase their active power outputs by highest amounts in the low and medium wind speeds. In order to increase the meaningfulness of such support, probability of different wind speeds is studied. Wind speed measurements used in this thesis are taken from a real wind farm with GE 2.75-103 model wind turbines between 01/01/2017 and 21/08/2017. Probability density function (PDF) of the measurements is given in Fig. 4.20. The wind speed measurements have a mean of 7.13 with a standard deviation of 3.85.

For a defined wind speed, the active power increase can be calculated by considering the Section 4.1. However, likelihood of such an increase can be calculated by integrating PDF over desired the wind speed range. This can also be calculated from the cumulative distribution function (CDF) of the measurements. In this case, CDFs of the wind speed range limits will be used. Wind Speed CDF is given in Fig. 4.21.

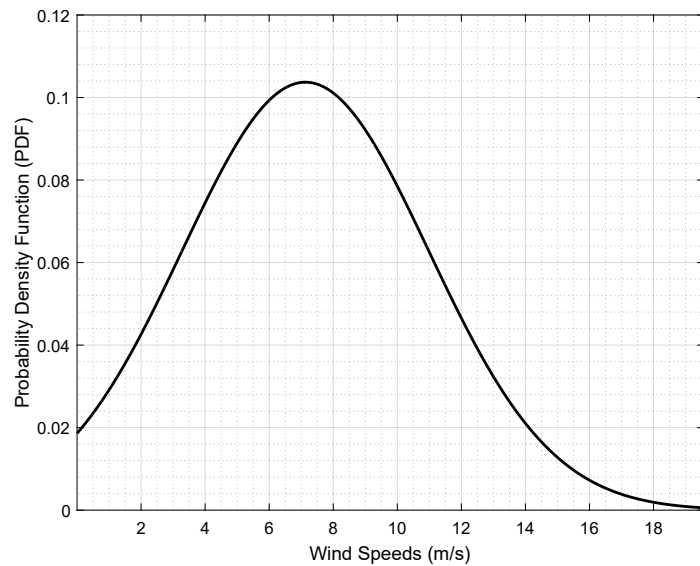


Figure 4.20: Probability Density Function of Measured Wind Speeds

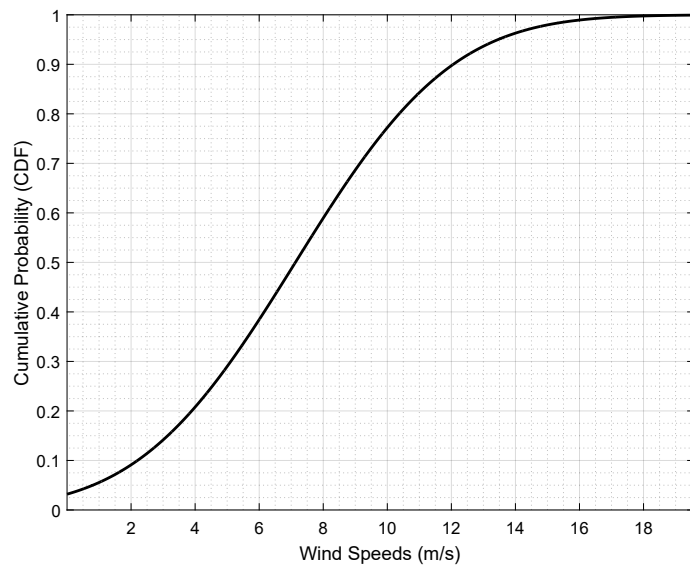


Figure 4.21: Cumulative Distribution Function of Measured Wind Speeds

CHAPTER 5

VALIDATION IN TEST CASE

5.1 P.M.Anderson 9 Bus Test Case

5.1.1 System Properties

In order to understand frequency dynamics better, P.M. Anderson test case has been used in the study. The single line diagram of the system is given in Fig. 5.1. The test case consists of three generators and three loads. Generators in the system are connected to 230 kV high voltage network with transformers.

The biggest generator in the system is a hydro power plant with a power rating of 247.5 MVA. The remaining ones are steam generators. The power ratings of the generators are given in Table 5.1.

Generators	Power Rating (MVA)	Plant Type
Gen 1	247.5	Hydro
Gen 2	192	Steam
Gen 3	128	Steam

Table 5.1: Generator Properties of Test System

The loads in the system are connected directly to the high voltage network. The active and reactive power ratings of the loads are listed in Table 5.2.

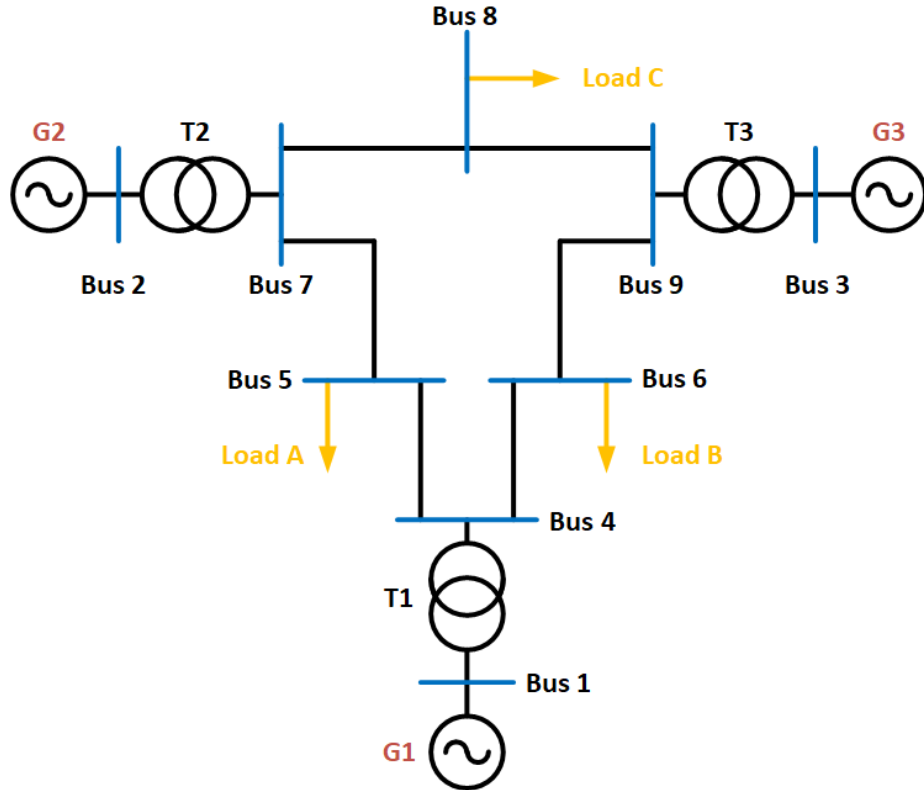


Figure 5.1: P.M.Anderson Test Case

Generators	Active Power (MW)	Reactive Power (MVAr)
Load A	125	50
Load B	90	30
Load C	100	35

Table 5.2: Load Properties of Test System

5.1.2 Load Flow Analysis for Base Case

Successful grid operation requires a load flow analysis in order to ensure that bus voltages are inside the allowed band and power flows are below the power carrying capabilities of the lines. Load flow results are given in Table 5.3.

Bus #	Bus Type	Voltage	Angle	Pg	Qg	P1	Q1
1	SL	1.04	0	71.65	27.05	0	0
2	PV	1.025	9.28	163	6.65	0	0
3	PV	1.025	4.66	85	-10.86	0	0
4	PQ	1.0258	-2.22	0	0	0	0
5	PQ	0.9956	-3.99	0	0	125	50
6	PQ	1.0126	-3.69	0	0	90	30
7	PQ	1.0258	3.72	0	0	0	0
8	PQ	1.0159	0.73	0	0	100	35
9	PQ	1.0323	1.97	0	0	0	0

Table 5.3: Load Flow Results in Base Case

Total System Load	315 MW
Generator Droop Settings	5%
Stored Kinetic Energy at Nominal Speed	3.305 GWs
Gen 1 Inertia Constant	9.5515 s
Gen 2 Inertia Constant	3.9216 s
Gen 3 Inertia Constant	2.7665 s

Table 5.4: System Dynamical Properties

5.1.3 Base Case Frequency Response for Additional Load Connection

It is obvious that power system networks experience high RoCoF when either high amount of generation trips or high amount of load connects to system. These two main event can be used in the simulation to create frequency disturbances. Since the simulation in Simulink environment slows down with the increasing amount of generators, the disturbances are created with load connections.

System dynamical properties are listed in Table 5.4. Power generation references are determined based on the load flow of powergui toolbox. Machine initialization toolbox is also used to initiate the state of generators in the system. However, the system does not start with the steady state. Still, system goes to steady state within

a few seconds. Frequency of the network is disturbed with a load connection in the $t=10$ seconds in order to observe the frequency stability of the system. For 10% load connection, a load of 31.5 MW is connected to system from Bus 6. Location of the additional load is depicted in Fig. 5.2.

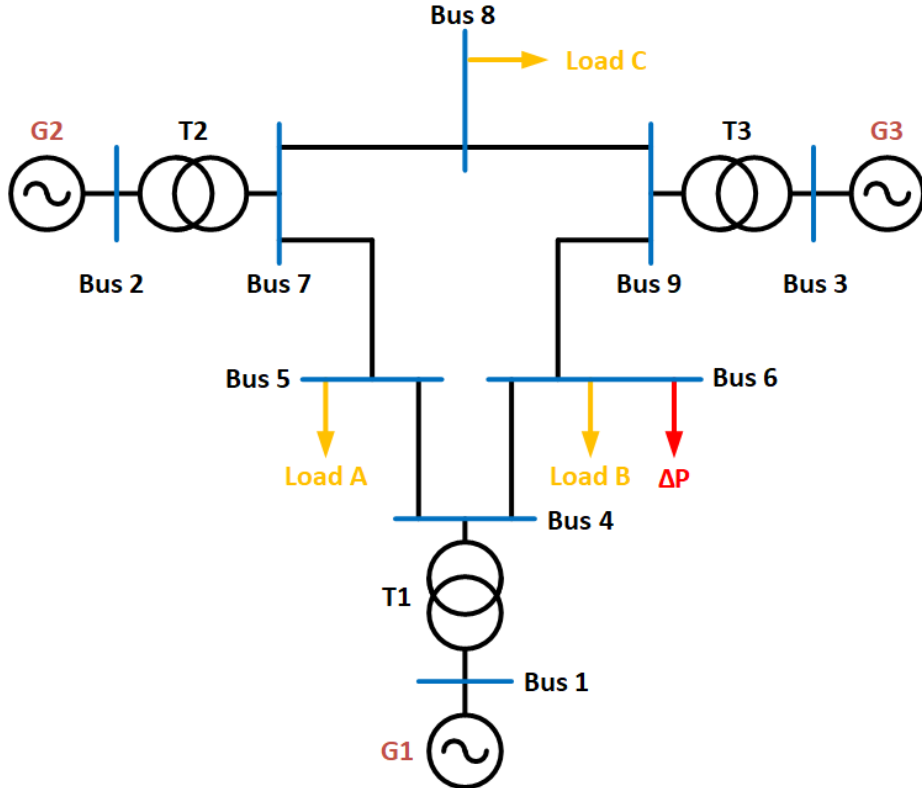


Figure 5.2: Location of the Additional Load

According to the 10% load connection to system, generator frequencies are shown in Fig. 5.3. As it can be seen from Fig. 5.3, rotor swings exists in the frequencies. However, the frequency of generator 1 is the most smooth one due to its huge inertia constant. Meanwhile, the generator 2 and generator 3 follow the frequency of generator 1 with higher rotor swings. In the system, frequency of Bus 1 can be assumed as constant throughout the network since the system is small enough to assume a single frequency. This assumption can be verified by comparing the frequencies in Buses 1, 5 and 6. Fig. 5.4 shows the frequency of the generator 1 frequency as well as the load frequencies captured with Simulink PLL block. The only difference is the instant following the load connection. The sharp frequency decline delays the PLL loop to capture the frequency.

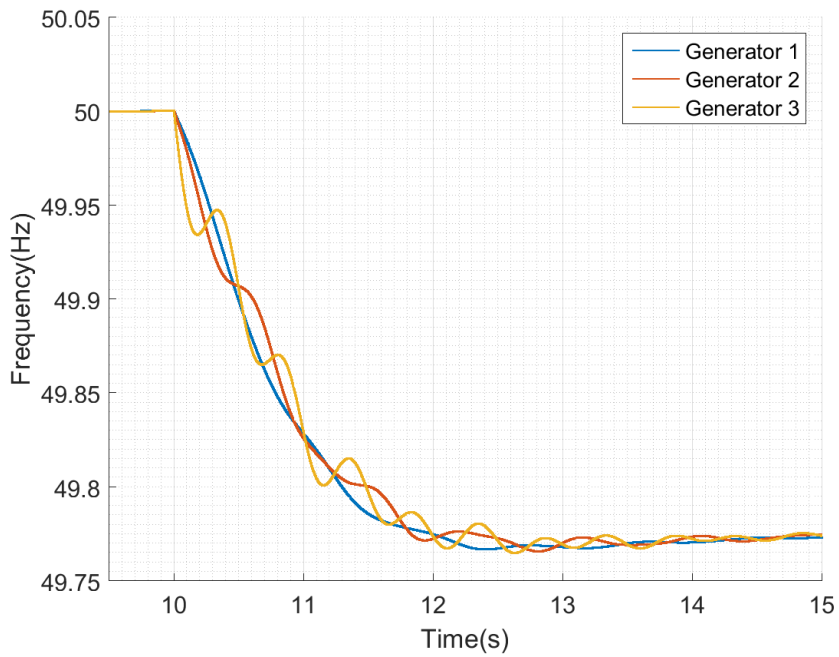


Figure 5.3: Generator Frequencies for 10% Load Connection

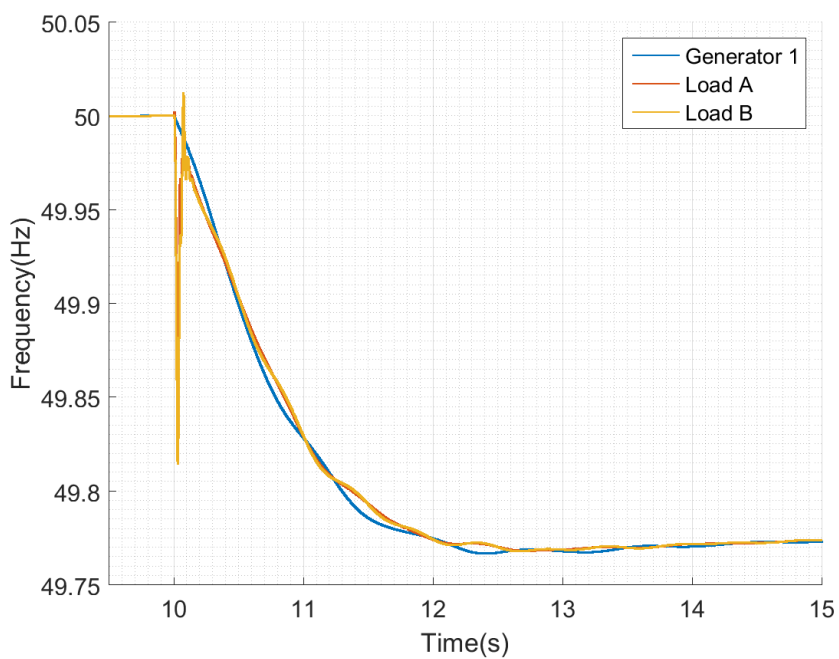


Figure 5.4: Frequencies in Generator 1, Load A and Load B

5.2 Modified Case

In this case, the P.M. Anderson test case is modified such that a wind farm consists of 20 wind turbine is connected to network. Wind farm is connected to Bus 5. Modified system is depicted in the Fig. 5.5. In this case, generator 2 and 3 are still assigned to same power values meanwhile generator 1 decreases its generation.

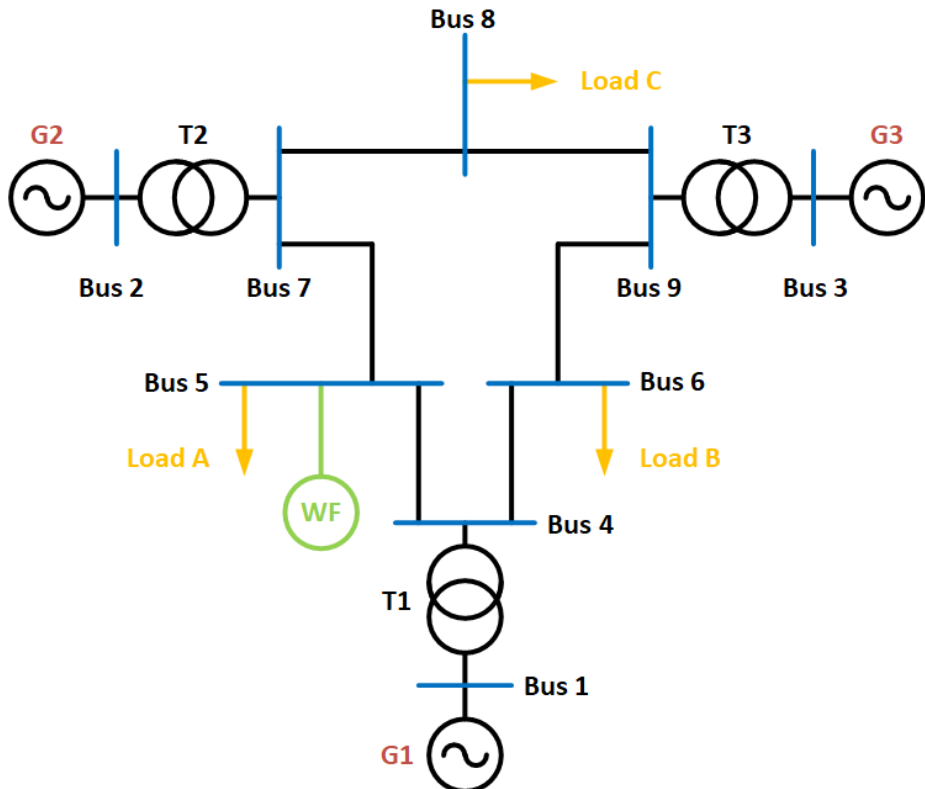


Figure 5.5: Modified System Single Line Diagram

5.2.1 Load Flow Analysis for Modified Case

Load flow analysis for modified case is listed in Table 5.5. The power injected from Bus 1 is decreased as expected. This can also be seen from the phase angle between 1 and 4. Phase angle difference between these buses decreased from 2.22° to 1.18° .

Bus #	Bus Type	Voltage	Angle	Pg	Qg	P1	Q1
1	SL	1.04	0	38.06	25.07	0	0
2	PV	1.025	11.33	163	6.65	0	0
3	PV	1.025	6.32	85	-10.86	0	0
4	PQ	1.0263	-1.18	0	0	0	0
5	PQ	0.9995	-1.54	0	0	125	50
6	PQ	1.0128	-2.43	0	0	90	30
7	PQ	1.0266	5.77	0	0	0	0
8	PQ	1.0164	2.62	0	0	100	35
9	PQ	1.0326	3.62	0	0	0	0

Table 5.5: Load Flow Results for Modified Case

5.2.2 Modified Case Frequency Response for Additional Load Connection

The modified base is very similar to the Base Case except for a wind farm located in Bus 5. The renewable energy system in this case can be considered as a negative load. Therefore, base case with decreased load is under discussion in this subsection. The same amount of load is taken into operation at Bus 6 and the frequency of the system is shown in Fig. 5.6.

Almost the same frequency response is observed in the system. The reason is that both systems have the same amount of stored kinetic energy. Another reason is the underutilization of the power system network. This can also be observed in the rate of change of frequencies in Fig. 5.7. Almost the same RoCoF values are observed in the system. This concludes that renewable energy penetration does not change frequency response of the system if the only change in the system is the inclusion of renewable energy system. Note that the renewable energy systems are intermittent energy sources. However, in this study, the source of the renewable energy system is assumed as constant. Therefore, the reason of frequency disturbance is load connection rather than the change in active power output of renewable systems.

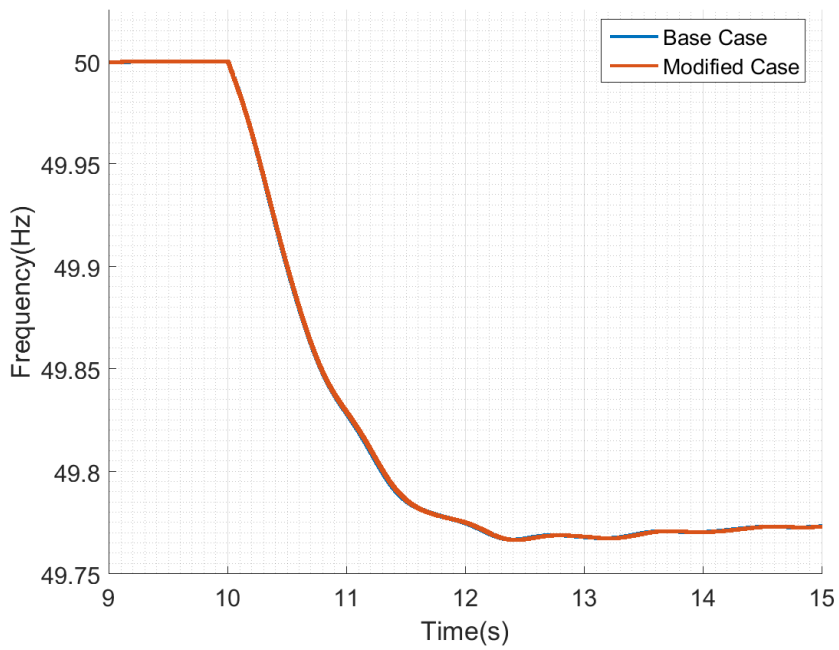


Figure 5.6: Comparison of Base Case and Modified Case Frequencies

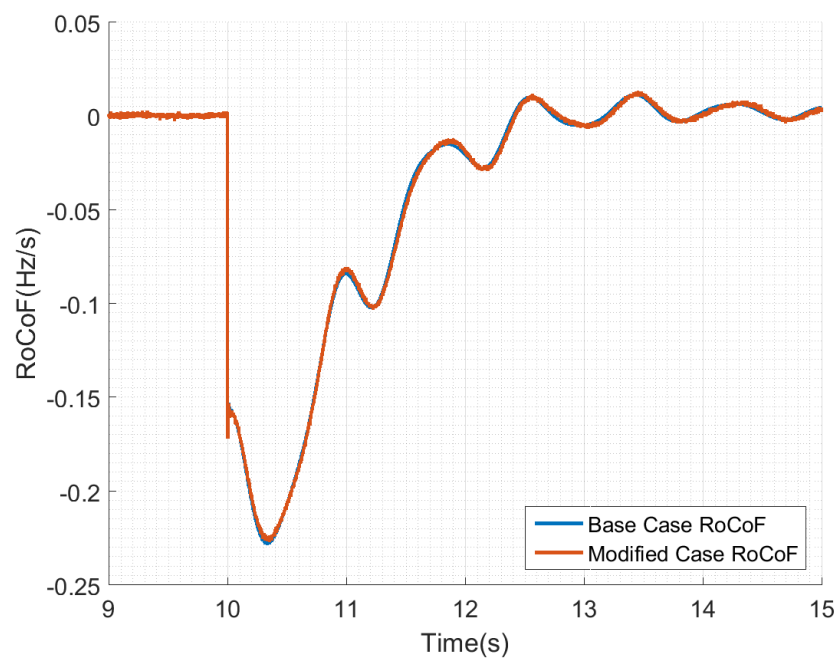


Figure 5.7: Comparison of Base Case and Modified Case Frequencies

5.3 Decommissioned Case

As seen in the Modified Case, the frequency response of the system does not change with renewable energy inclusion. However, it is inevitable that renewable energy systems will replace the conventional units in future. In this case, the smallest generator, generator 3, will be decommissioned. The decommissioned case diagram is shown in Fig. 5.8.

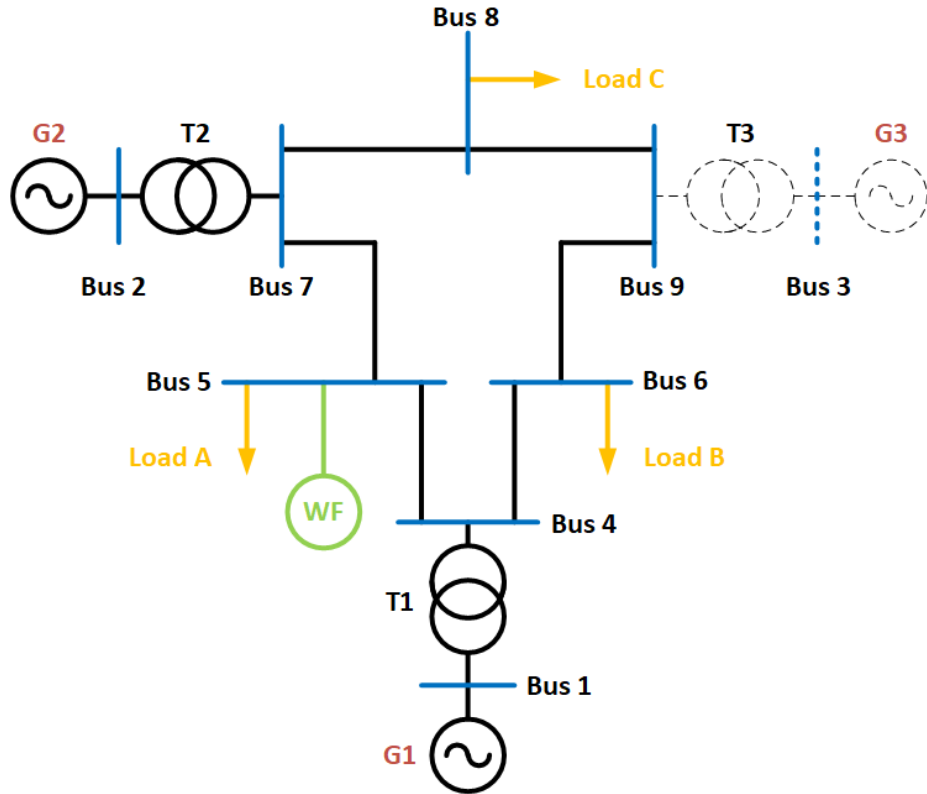


Figure 5.8: Comparison of Base Case and Modified Case Frequencies

Since the generator 3 is out of service, the stored kinetic energy is decreased in the system. Decommissioned system dynamical properties are updated and given in Table 5.6.

5.3.1 Load Flow Analysis for Decommissioned Case

Since the generator 3 is out of service, generator 1 loading will be increased. Load flow analysis for decommissioned case is given in Table 5.7.

Total System Load	315 MW
Generator Droop Settings	5%
Stored Kinetic Energy at Nominal Speed	3.004 GWs
Gen 1 Inertia Constant	9.5515 s
Gen 2 Inertia Constant	3.9216 s

Table 5.6: System Dynamical Properties

Bus #	Bus Type	Voltage	Angle	Pg	Qg	Pl	Ql
1	SL	1.04	0	121.76	16.26	0	0
2	PV	1.025	4.18	163	0.65	0	0
4	PQ	1.0332	-3.74	0	0	0	0
5	PQ	1.0083	-5.63	0	0	125	50
6	PQ	1.0224	-7.65	0	0	90	30
7	PQ	1.0294	-1.36	0	0	0	0
8	PQ	1.0207	-5.82	0	0	100	35

Table 5.7: Load Flow Results for Decommissioned Case

5.3.2 Decommissioned Case Frequency Response for Additional Load Connection

Same amount of additional load is taken into operation from Bus 6. System frequency response is observed and compared to Base Case and Modified Case in Fig. 5.9. As soon from the figure, the frequency nadir decreased from 49.77Hz to 49.65Hz. This is due to the decrease in the stored kinetic energy in the system. Due to the decommission of generator 3, the frequency decreases steeper following to load connection. This can also be observed RoCoF comparison given in Fig. 5.10.

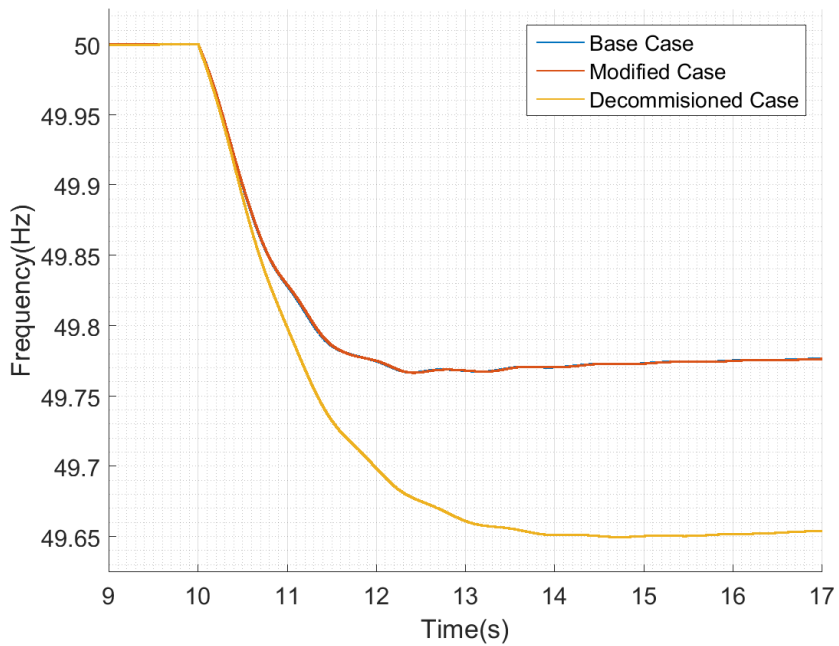


Figure 5.9: Comparison of Base Case, Modified Case and Decommissioned Case Frequency Responses

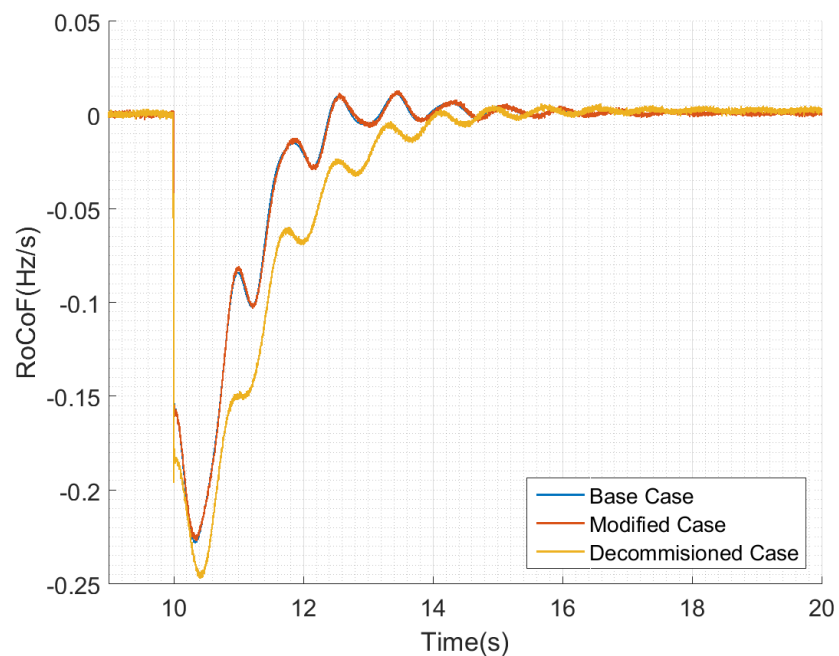


Figure 5.10: Comparison of Base Case, Modified Case and Decommissioned Case RoCoFs

CHAPTER 6

EVALUATION OF FAST INERTIAL RESPONSE AND SYNTHETIC INERTIA IMPLEMENTATION

6.1 FAST INERTIAL RESPONSE

6.2 SYNTHETIC INERTIA IMPLEMENTATION

6.3 FUTURE WORK

REFERENCES

- [1] Eurostat, “Renewable energy in the EU-newsrelease,” Tech. Rep. January, 2018.
- [2] European Commission; and IRENA International Renewable Energy Agency, “Renewable Energy Prospects for the European Union,” Tech. Rep. February, 2018.
- [3] IRENA, “A Renewable Energy Roadmap,” Tech. Rep. June, 2014.
- [4] P. Kundur, *Power System Stability and Control*. McGraw-Hill, Inc.
- [5] J. Eto, J. Undrill, P. Mackin, R. Daschmans, B. Williams, B. Haney, R. Hunt, J. Ellis, H. Illian, C. Martinez, M. OMalley, K. Coughlin, and K. Hamachi-LaCommare, “Use of Frequency Response Metrics to Assess the Planning and Operating Requirements for Reliable Integration of Variable Renewable Generation.” 2010.
- [6] International Renewable Energy Agency (IRENA), *IRENA (2018), Renewable capacity statistics 2018*. 2018.
- [7] International Renewable Energy Agency, *Renewable Energy Statistics 2017*. 2017.
- [8] European Commission, “Communication from the Commission to the European Parliament, the Council, the European economic and social Committee and the Committee of the Regions - 2020 by 2020 - Europe’s climate change opportunity,” *COM (2008) 30 final*, p. Brussels, 2008.
- [9] European Parliament, “Directive 2009/28/EC of the European Parliament and of the Council of 23 April 2009,” *Official Journal of the European Union*, vol. 140, no. 16, pp. 16–62, 2009.
- [10] REN21, *Renewables Global Futures Report*. 2017.

- [11] H. Klinge Jacobsen and E. Zvingilaite, “Reducing the market impact of large shares of intermittent energy in Denmark,” *Energy Policy*, vol. 38, no. 7, pp. 3403–3413, 2010.
- [12] M. Zipf and D. Most, “Impacts of volatile and uncertain renewable energy sources on the German electricity system,” *International Conference on the European Energy Market, EEM*, 2013.
- [13] A. Ipakchi and F. Albuyeh, “Grid of the future,” *IEEE Power and Energy Magazine*, vol. 7, no. 2, pp. 52–62, 2009.
- [14] D. Gautam, L. Goel, R. Ayyanar, V. Vittal, and T. Harbour, “Control strategy to mitigate the impact of reduced inertia due to doubly fed induction generators on large power systems,” *IEEE Transactions on Power Systems*, vol. 26, no. 1, pp. 214–224, 2011.
- [15] E. Muljadi, V. Gevorgian, and M. Singh, “Understanding Inertial and Frequency Response of Wind Power Plants Preprint,” *2012 IEEE Power Electronics and Machines in Wind Applications (PEMWA)*, no. July, pp. 1–8, 2012.
- [16] J. Van De Vyver, J. D. M. De Kooning, B. Meersman, L. Vandeven, and T. L. Vandoorn, “Droop Control as an Alternative Inertial Response Strategy for the Synthetic Inertia on Wind Turbines,” *IEEE Transactions on Power Systems*, vol. 31, no. 2, pp. 1129–1138, 2016.
- [17] G. Lalor, J. Ritchie, S. Rourke, D. Flynn, and M. O’Malley, “Dynamic frequency control with increasing wind generation,” *IEEE Power Engineering Society General Meeting, 2004.*, pp. 1–6, 2004.
- [18] J. Ekanayake, “Control of DFIG wind turbines,” *Power Engineer*, vol. 17, no. 1, pp. 28–32, 2003.
- [19] J. Ekanayake and N. Jenkins, “Comparison of the response of doubly fed and fixed-speed induction generator wind turbines to changes in network frequency,” *IEEE Transactions on Energy Conversion*, vol. 19, no. 4, pp. 800–802, 2004.
- [20] J. Morren, S. de Haan, W. Kling, and J. Ferreira, “Wind Turbines Emulating Inertia and Supporting Primary Frequency Control,” *IEEE Transactions on Power Systems*, vol. 21, no. 1, pp. 433–434, 2006.

- [21] J. Morren, J. Pierik, and S. W. de Haan, “Inertial response of variable speed wind turbines,” *Electric Power Systems Research*, vol. 76, no. 11, pp. 980–987, 2006.
- [22] T. Ackermann, *Wind Power in Power Systems Wind Power in Power Systems Edited by*, vol. 8. 2005.
- [23] S. Heier, *Grid Integration of Wind Energy*. 3 ed., 1998.
- [24] Q. Wang and L. Chang, “An Intelligent Maximum Power Extraction Algorithm for Inverter-Based Variable Speed Wind Turbine Systems,” *IEEE Transactions on Power Electronics*, vol. 19, no. 5, pp. 1242–1249, 2004.
- [25] M. Barakati, M. Kazerani, and D. Aplevich, “Maximum Power Tracking Control for a Wind Turbine System Including a Matrix,” vol. 24, no. Mc, p. 4244, 2009.
- [26] T. Thriringer and J. Linders, “Control by Variable Rotor Speed of a Fixed Pitch Wind,” *IEEE Transactions on Energy*, vol. 8, no. 3, pp. 520–526, 1993.
- [27] R. C.A., V. G., A. D., A. A., and M. M., “Prophylaxis in adults hemophiliac patients with severe arthropathy,” *Journal of Thrombosis and Haemostasis*, vol. 11, p. 1081, 2013.
- [28] W. Lu and B. T. Ooi, “Multiterminal LVDC system for optimal acquisition of power in wind-farm using induction generators,” *IEEE Transactions on Power Electronics*, vol. 17, no. 4, pp. 558–563, 2002.
- [29] Q. Zeng, L. Chang, and R. Shao, “Fuzzy-logic-based maximum power point tracking strategy for PMSG variable-speed wind turbine generation systems,” *Canadian Conference on Electrical and Computer Engineering*, no. 1, pp. 405–409, 2008.
- [30] W. M. Lin, C. M. Hong, and C. H. Chen, “Neural-network-based MPPT control of a stand-alone hybrid power generation system,” *IEEE Transactions on Power Electronics*, vol. 26, no. 12, pp. 3571–3581, 2011.
- [31] H. Polinder, J. A. Ferreira, B. B. Jensen, A. B. Abrahamsen, K. Atallah, and R. a. McMahon, “Trends in Wind Turbine Generator Systems,” *IEEE Journal of*

Emerging and Selected Topics in Power Electronics, vol. 1, no. 3, pp. 174–185, 2013.

- [32] T. P. Chen, “Dual-modulator compensation technique for parallel inverters using space-vector modulation,” *IEEE Transactions on Industrial Electronics*, vol. 56, no. 8, pp. 3004–3012, 2009.
- [33] M. P. Kazmierkowski, R. Krishnan, and F. Blaabjerg, *Control in Power Electronics—Selected Problems*. New York: Academic, 2002.
- [34] F. Blaabjerg, R. Teodorescu, M. Liserre, and A. V. Timbus, “Overview of control and grid synchronization for distributed power generation systems,” *IEEE Transactions on Industrial Electronics*, vol. 53, no. 5, pp. 1398–1409, 2006.
- [35] M. Chinchilla, S. Arnaltes, and J. C. Burgos, “Control of permanent-magnet generators applied to variable-speed wind-energy systems connected to the grid,” *IEEE Transactions on Energy Conversion*, vol. 21, no. 1, pp. 130–135, 2006.
- [36] T. Orłowska-Kowalska, F. Blaabjerg, and J. Rodríguez, *Advanced and intelligent control in power electronics and drives*. 2014.
- [37] F. M. Gonzalez-longatt, “Activation Schemes of Synthetic Inertia Controller on Full Converter Wind Turbine (Type 4),” no. Type 4, 2015.

APPENDIX A

EK A

A.1 Örnek Kısım

Kısım içine yazılacaklar...